Gold(III)-Mediated Insertion of Se and Te into Au–P Bonds: *En route* to Diphosphane Chalcogenides and σ-Hole Modulation

Juan Carlos Pérez-Sánchez,[a,b] Jesús Moradell,[a] Juan V. Alegre-Requena,[a] Raquel P. Herrera,[b] and M. Concepción Gimeno*

[a]Departamento de Química Inorgánica, Instituto de Síntesis Química y Catálisis Homogénea (ISQCH), Consejo Superior de Investigaciones Científicas (CSIC)-University of Zaragoza, Pedro Cerbuna 12, 50009, Zaragoza, Spain.

[b]Departamento de Química Orgánica, Instituto de Síntesis Química y Catálisis Homogénea (ISQCH), Consejo Superior de Investigaciones Científicas (CSIC)-University of Zaragoza, Pedro Cerbuna 12, 50009, Zaragoza, Spain.

gimeno@unizar.es

Table of Contents

1. General Information

General Considerations and Materials: All experiments and manipulations were carried under air unless otherwise stated. All solvents were used as received. All chemical reagents were purchased from commercial suppliers and used as received. The starting materials $[Au(C_6F_5)_2(dppm)][ClO_4]$ (dppm = bis(diphenylphosphane)methane),[1] [{Au(C^C)(dppm)][ClO_4] (C^C = 4,4′-di-tert-butyl-1,1′-biphenyl),[2] $TeP(^iPr)_3$,[3] and $SeP(^iPr)_3$[3] were prepared according to published procedures. All other reagents were commercially available and were used without further purification.

NMR Information: ^1H, ^{19}F, $^{31}P\{^1H\}$, ^{125}Te, ^{77}Se NMR spectra were recorded on a Bruker Avance 300 or 400 spectrometers at the indicated frequencies at 298.15K, unless otherwise stated. Chemical shifts are reported in ppm and referenced to the residual ^1H signal of the deuterated solvent as internal reference (^1H NMR), external H_3PO_4 85% ($^{31}P\{^1H\}$ NMR), external $CFCl_3$ (^{19}F NMR), external Ph_2Te_2 (^{125}Te NMR, 0.1 M in CD_2Cl_2, δ_{Te} = 420.8 ppm) and external Ph_2Se_2 (^{77}Se NMR, liquid, δ_{Se} = 463.0 ppm). When it is not possible to directly record the 1D spectra of ^{125}Te or ^{77}Se, chemical shift values are obtained indirectly through a 2D HMQC ^1H-^{125}Te or ^1H-^{77}Se experiment (HMQC = Heteronuclear Multiple Quantum Correlation), *via* a $^3J_{HTe}$ or $^3J_{HSe}$ with a fixed value of 10 Hz. Multiplicity of the observed signals is indicated as follows: s = singlet, br s = broad singlet, d = doublet, dd = doublet of doublets, t = triplet, vt = virtual triplet, d sept = doublet of septuplets, m = multiplet. *J* values are given in Hz.

HRMS and Elemental Analysis Information: High resolution mass spectra of complexes were acquired on a Bruker MicroTOF-Q (ESI+) spectrometer. Elemental analyses were carried out using a Perkin Elmer 2400 CHNS/O Series II microanalyzer.

Crystallography: Crystals suitable for X-ray studies were obtained by vapor diffusion of diethyl ether over a solution of the compound in dichloromethane. Crystals were mounted on a MiTeGen Crystal micromount and transferred to the cold gas stream of a Bruker D8 VENTURE diffractometer. Data were collected using monochromated MoK α radiation (λ = 0.71073 Å). Scan type ω. Absorption correction based on multiple scans were applied with the program SADABS.[4] The structures were refined on F^2 using the program SHELXL-18.[5] All non-hydrogen atoms were refined anisotropically. Hydrogen atoms were included using a riding model. Images of the crystal structures were generated with Mercury 2021.3.0.[6] CCDC deposition numbers 2522544 (**1**), 2522545 (**3**) and 2522546 (**5**) contain supplementary crystallographic data. This data can be obtained free of charge by The Cambridge Crystallography Data Center.

2. Experimental Procedures

Synthesis of Complex $[Au(C_6F_5)_2(TePPh_2CH_2PPh_2)][ClO_4]$ (1)

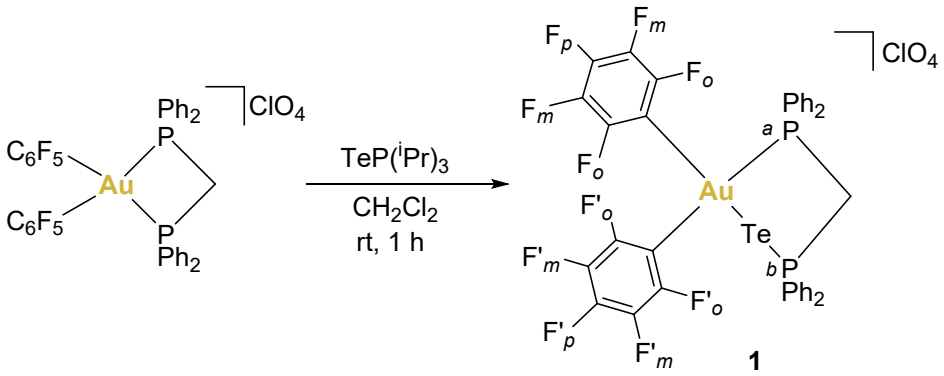

To a Schlenk flask equipped with a stirring bar, under air, was added $TeP(^iPr)_3$ (28.8 mg, 0.1 mmol) and 20 mL of CH_2Cl_2. Then $[Au(C_6F_5)_2(dppm)][ClO_4]$ (101.5 mg, 0.1 mmol) was added, and the resulting bright yellow solution was stirred for 1 hour. After this time, the solution was concentrated under reduced pressure to *ca.* 1 mL. Then, diethyl ether (10 mL) was added to precipitate a yellow solid which was purified through washings with diethyl ether (2 x 5 mL) and dried under vacuum. Yield (93.1 mg, 54%).

^{1}H NMR (400 MHz, CD_2Cl_2, 25 °C) δ_H (ppm): 7.85 – 7.73 (m, 4H, Ph), 7.61 – 7.32 (m, 16H, Ph), 5.93 (vt, $^2J_{H,P}$ = 12.5 Hz, 2H, CH_2).

^{31}P{^{1}H} NMR (162 MHz, CD_2Cl_2, 25 °C) δ_P (ppm): 30.6 (dt, $^2J_{P,P}$ = 50.6 Hz, $^4J_{P,F}$ = 10.7 Hz, 1P, P_a), -2.0 (d, $^2J_{P,P}$ = 50.9 Hz, 1P, P_b).

^{19}F NMR (376 MHz, CD_2Cl_2, 25 °C) δ_F (ppm): -117.3 – -117.5 (m, 2F, F'_o), -122.5 – -122.7 (m, 2F, F_o), -154.7 (t, J = 19.6 Hz, 1F, F'_p), -155.8 (t, J = 19.7 Hz, 1F, F_p), -159.9 (m, 2F, F_m), -160.3 (m, 2F, F'_m).

^{125}Te NMR (126 MHz, CD_2Cl_2, 25 °C) δ_{Te} (ppm): 162.5 (dd, $^1J(^{125}Te\text{-}^{31}P)$ = 1156.8 Hz, $^3J(^{125}Te\text{-}^{31}P)$ = 53.2 Hz), 1Te, *Te*P(Ph)$_2$).

HRMS (ESI/QTOF) m/z calcd. for $C_{37}H_{22}AuF_{10}P_2Te$: 1044.9760 $[M]^+$; found 1044.9755.

Elemental analysis (%) calcd. for $C_{37}H_{22}AuClF_{10}O_4P_2Te$, C: 38.90, H: 1.94; found C: 38.59, H: 1.97.

Synthesis of Complex [Au(C^C)(TePPh$_2$CH$_2$PPh$_2$)][ClO$_4$] (2)

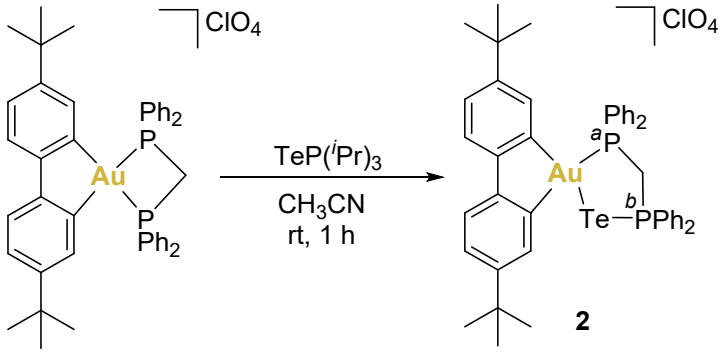

To a Schlenk flask equipped with a stirring bar, under argon, was added TeP(^{i}Pr)$_3$ (14.4 mg, 0.05 mmol) and 20 mL of dry and degassed CH_3CN. Then [Au(C^C)(dppm)][ClO_4] (47.3 mg, 0.05 mmol) was added, and the resulting bright yellow solution was stirred for 1 hour at room temperature. After this time, the solution was concentrated under reduced pressure to *ca.* 1 mL. Then, diethyl ether (10 mL) was added to precipitate a yellow solid which was dried under vacuum. Yield (36.0 mg, 68%).

^{1}H NMR (400 MHz, CD_2Cl_2, 25 °C) δ_H (ppm): 7.98 (dt, J = 9.9, 2.2 Hz, 1H), 7.87 – 7.30 (m, 23H), 7.14 (dd, J = 8.0, 1.8 Hz, 1H), 6.76 (dd, J = 4.3, 1.8 Hz, 1H), 5.55 (dd, $^2J_{H,P}$ = 12.8 Hz, $^2J_{H,P}$ = 11.7 Hz, 2H, CH_2), 1.39 (s, 9H, C(CH_3)$_3$), 0.65 (s, 9H, C(CH_3)$_3$).

^{31}P{^{1}H} NMR (162 MHz, CD_3CN, 25 °C) δ_P (ppm): 35.8 (d, $^2J_{P,P}$ = 49.0 Hz, 1P, P_a), –9.6 (d, $^2J_{P,P}$ = 48.7 Hz, 1P, P_b).

^{125}Te NMR (126 MHz, CD_3CN, 25 °C) δ_{Te} (ppm): –10.7 (1Te, *Te*P(Ph)$_2$).

HRMS (ESI/QTOF) m/z calcd. for $C_{45}H_{46}AuP_2Te$ 975.1797 $[M]^+$; found 975.1794.

Synthesis of Complex [Au(C$_6$F$_5$)$_2$(SePPh$_2$CH$_2$PPh$_2$)][ClO$_4$] (3)

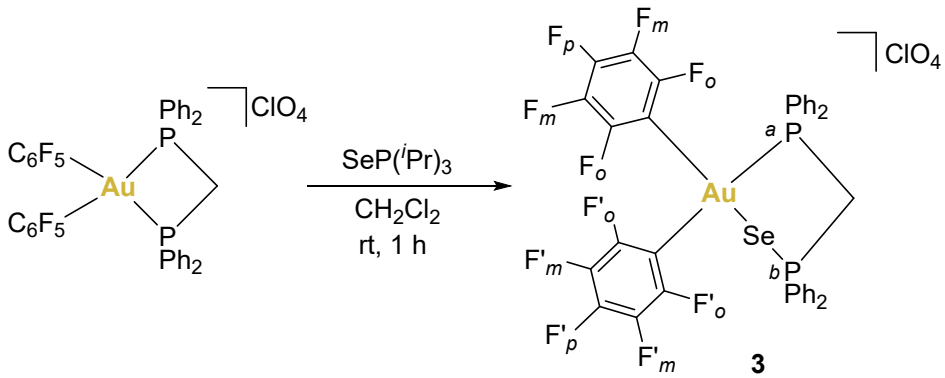

To a Schlenk flask equipped with a stirring bar, under air, was added SeP(^{i}Pr)$_3$ (23.9 mg, 0.1 mmol) and 20 mL of CH_2Cl_2. Then [Au(C$_6$F$_5$)$_2$(dppm)][ClO_4] (101.5 mg, 0.1 mmol) was added, and the resulting bright yellow solution was stirred for 1 hour. After this time, the solution was concentrated under reduced pressure to *ca.* 1 mL. Then, diethyl ether (10 mL) was added to precipitate a white solid which was purified through washings with diethyl ether (2 x 5 mL) and dried under vacuum. Yield (30.2 mg, 60%).

^{1}H NMR (400 MHz, CD_2Cl_2, 25 °C) δ_H (ppm): 7.97 – 7.75 (m, 4H, Ph), 7.71 – 7.30 (m, 16H, Ph), 5.45 (vt, $^{2}J_{H,P}$ = 12.0 Hz, 2H, CH_2).

^{31}P{^{1}H} NMR (162 MHz, CD_2Cl_2, 25 °C) δ_P (ppm): 41.9 (d, $^{2}J_{P,P}$ = 40.8 Hz, 1P, P_b), 30.7 (dp, $^{2}J_{P,P}$ = 40.5 Hz, $^{4}J_{P,F}$ = 10.7 Hz, 1P, P_a).

^{19}F NMR (376 MHz, CD_2Cl_2, 25 °C) δ_F (ppm): -119.7 – -120.0 (m, 2F, F'_o), -121.9 – -122.5 (m, 2F, F_o), -154.7 (t, $^{3}J_{F,F}$ = 19.6 Hz, 1F, F'_p), -155.1 (t, $^{3}J_{F,F}$ = 19.7 Hz, 1F, F_p), -159.6 (m, 2F, F_m), -160.3 (m, 2F, F'_m).

^{77}Se NMR (76 MHz, CD_2Cl_2, 25 °C) δ_{Se} (ppm): 70.4 (d, $^{1}J(^{77}Se\text{-}^{31}P)$ = 484.4 Hz, 1Se, *Se*P(Ph)$_2$).

HRMS (ESI/QTOF) m/z calcd. for $C_{37}H_{22}AuF_{10}P_2Se$: 994.9862 $[M]^+$; found 994.9836.

Elemental analysis (%) calcd. for $C_{37}H_{22}AuClF_{10}O_4P_2Se$, C: 40.53, H: 2.03; found C: 40.32, H: 1.99.

Synthesis of Complex [Au(C^C)(SePPh$_2$CH$_2$PPh$_2$)][ClO$_4$] (4)

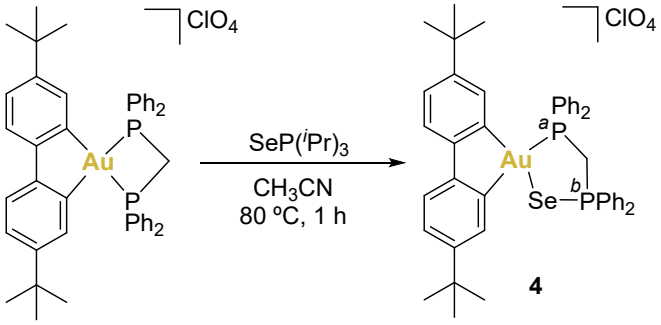

To a Schlenk flask equipped with a stirring bar, under argon, was added SeP(^{i}Pr)$_3$ (12.0 mg, 0.05 mmol) and 20 mL of dry and degassed CH_3CN. Then [Au(C^C)(dppm)][ClO_4] (47.3 mg, 0.05 mmol) was added, and the resulting solution was stirred for 1 hour at 80 °C. After this time, the solution was concentrated under reduced pressure to *ca.* 1 mL. Then, diethyl ether (10 mL) was added to precipitate a pale-yellow solid which was dried under vacuum. Yield (36.0 mg, 70%).

^{1}H NMR (400 MHz, CD_3CN, 25 °C) δ_H (ppm): 8.16 (dt, J = 9.8, 2.0 Hz, 1H, C^C), 7.87 – 7.26 (m, 23H, C^C + PPh$_2$), 7.13 (dd, J = 8.0, 1.8 Hz, 1H, C^C), 6.82 (dd, J = 4.1 Hz, 1.8 Hz, 1H, C^C), 5.04 (vt, $^{2}J_{H,P}$ = 11.8 Hz, 2H, CH_2), 1.37 (s, 9H, C(CH_3)$_3$), 0.64 (s, 9H, C(CH_3)$_3$).

^{31}P{^{1}H} NMR (162 MHz, CD_3CN, 25 °C) δ_P (ppm): 35.4 (d, $^{2}J_{P,P}$ = 42.8 Hz, 1P, P_b), 32.3 (d, $^{2}J_{P,P}$ = 42.9 Hz, 1P, P_a).

^{77}Se NMR (76 MHz, CD_3CN, 25 °C) δ_{Se} (ppm): –11.7 (d, $^{1}J(^{77}Se\text{-}^{31}P)$ = 511.9 Hz, 1Se, *Se*P(Ph)$_2$).

HRMS (ESI/QTOF) m/z calcd. for $C_{45}H_{46}AuP_2Se$ 925.1900 $[M]^+$; found 925.1917.

Synthesis of Phosphonium Chalcogenides 5 and 6

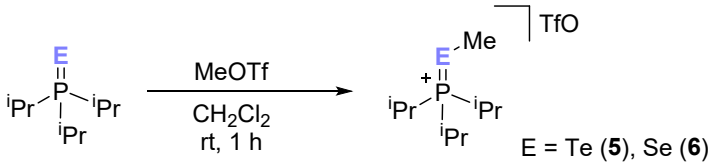

To a Schlenk flask equipped with a stirring bar, under argon, TeP(^{i}Pr)$_3$ (28.8 mg, 0.1 mmol, for **5**) or SeP(^{i}Pr)$_3$ (28.8 mg, 0.1 mmol, for **6**) was dissolved in 20 mL of dry and degassed CH_2Cl_2. Then methyl trifluoromethanesulfonate (24.6 mg, 17 µL, 0.15 mmol) was added, and the resulting solution was stirred for 1 hour at room temperature. After this time, the solution was concentrated under reduced pressure to *ca.* 1 mL. Then, diethyl ether (10 mL) was added to precipitate a white solid which was dried under vacuum.

Compound 5, yield (38.1 mg, 85%):

^{1}H NMR (400 MHz, CD_2Cl_2, 25 °C) δ_H (ppm): 2.72 (d sept, $^2J_{H,P}$ = 9.4 Hz, $^3J_{H,H}$ = 7.1 Hz, 3H, C*H*(CH$_3$)), 2.32 (d, $^3J_{H,P}$ = 8.0 Hz, 3H, PTe(C*H*$_3$)), 1.43 (dd, $^3J_{H,P}$ = 18.2, $^3J_{H,H}$ = 7.1 Hz, 18H, CH(C*H*$_3$)).

^{31}P{^{1}H} NMR (162 MHz, CD_2Cl_2, 25 °C) δ_P (ppm): 52.6 (s, 1P, *P*(^{i}Pr)$_3$, ^1J(^{31}P-^{125}Te) = 1092.9 Hz).

^{19}F NMR (376 MHz, CD_2Cl_2, 25 °C) δ_F (ppm): –78.9 (s, 3F, C*F*$_3$SO$_3^-$)

^{125}Te NMR (126 MHz, CD_2Cl_2, 25 °C) δ_{Se} (ppm): –114.6 (d, ^1J(^{125}Te-^{31}P) = 1110.1 Hz, 1Te, *Te*P(^{i}Pr)$_3$).

HRMS (ESI/QTOF) m/z calcd. for $C_{10}H_{24}PTe$ 306.0678 $[M]^+$; found 305.0714.

Compound 6, yield (32.7 mg, 81%):

^{1}H NMR (400 MHz, CD_2Cl_2, 25 °C) δ_H (ppm): 2.93 (d sept, $^2J_{H,P}$ = 9.2 Hz, $^3J_{H,H}$ = 7.1 Hz, 3H, C*H*(CH$_3$)), 2.46 (d, $^3J_{H,P}$ = 9.7 Hz, 3H, PSe(C*H*$_3$)), 1.47 (dd, $^3J_{H,P}$ = 18.2, $^3J_{H,H}$ = 7.1 Hz, 18H, CH(C*H*$_3$)).

^{31}P{^{1}H} NMR (162 MHz, CD_2Cl_2, 25 °C) δ_P (ppm): 73.4 (s, 1P, *P*(^{i}Pr)$_3$, ^1J(^{31}P-^{77}Se) = 439.2 Hz).

^{19}F NMR (376 MHz, CD_2Cl_2, 25 °C) δ_F (ppm): –78.9 (s, 3F, C*F*$_3$SO$_3^-$)

^{77}Se NMR (76 MHz, CD_2Cl_2, 25 °C) δ_{Se} (ppm): –79.2 (d, ^1J(^{77}Se-^{31}P) = 439.2 Hz, 1Se, *Se*P(^{i}Pr)$_3$).

HRMS (ESI/QTOF) m/z calcd. for $C_{10}H_{24}PSe$ 255.0781 $[M]^+$; found 255.0826.

3. NMR Spectral Data

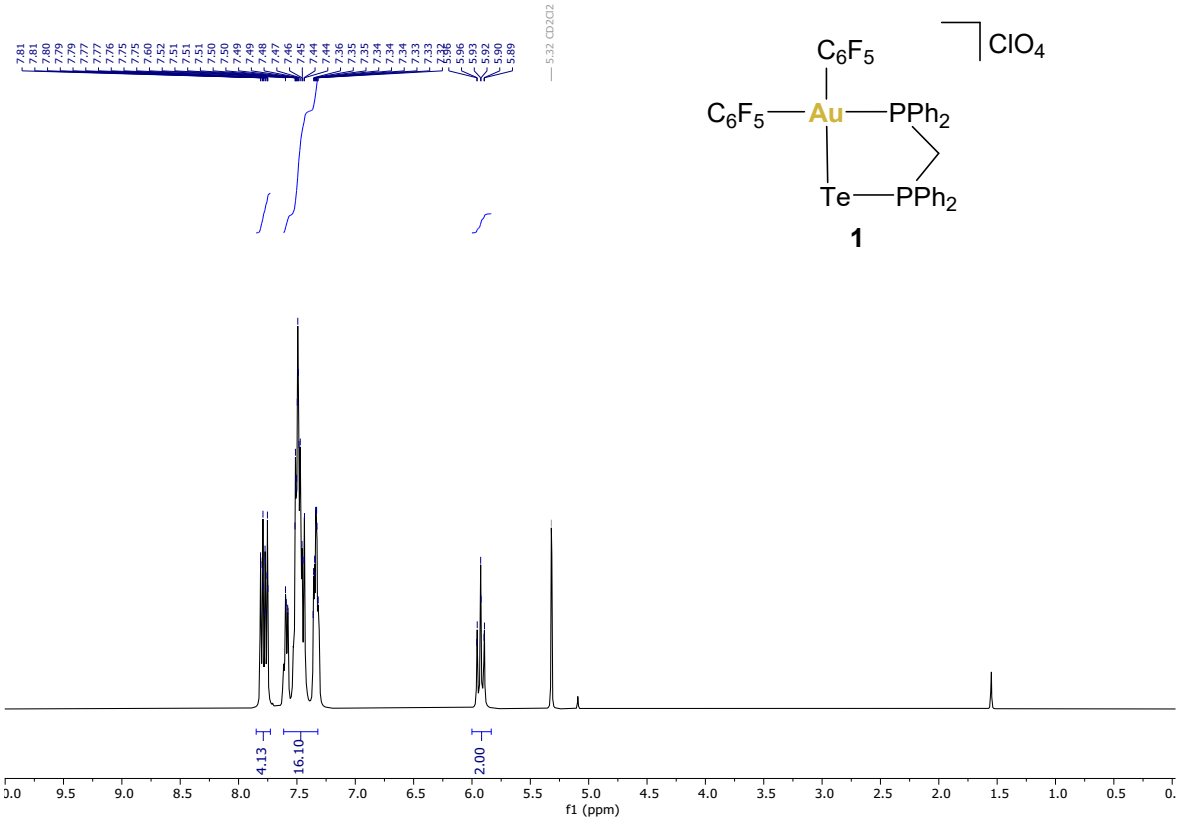

Figure S1. ^{1}H NMR (400 MHz, CD_2Cl_2, 25 °C) spectrum of complex **1**.

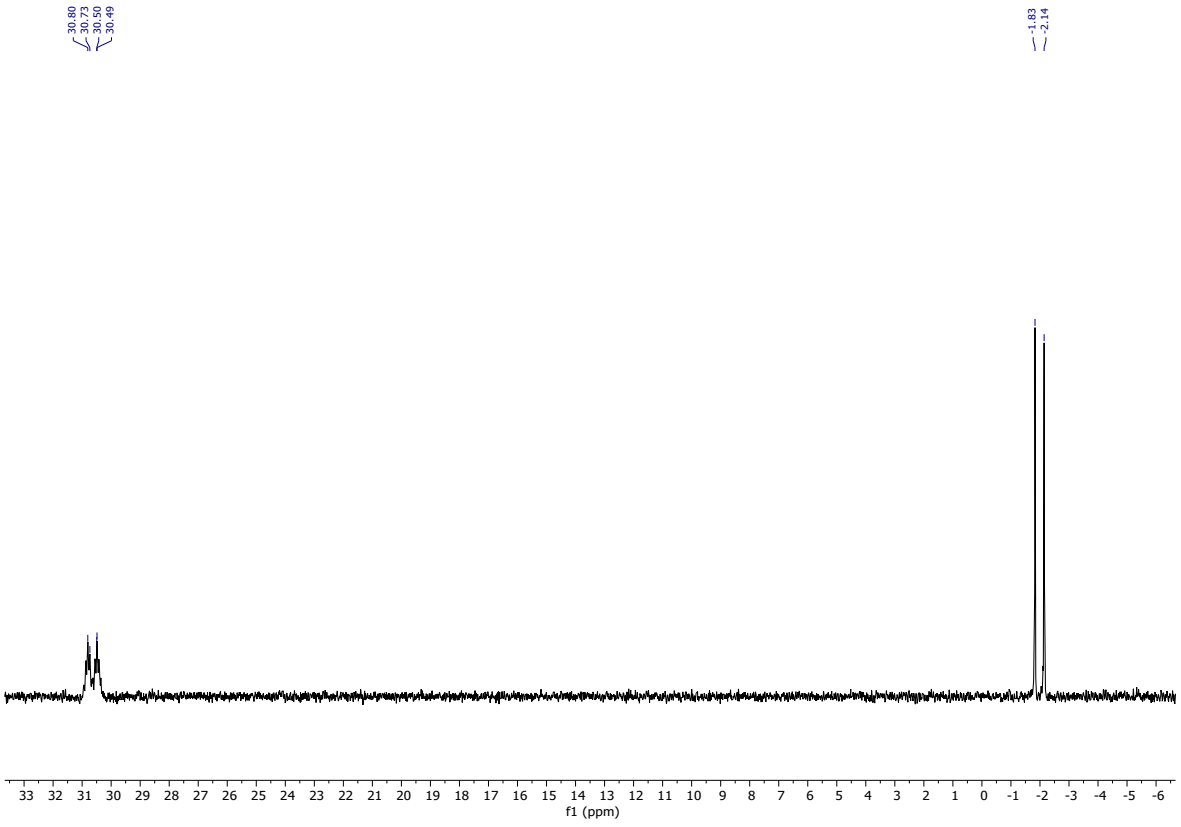

Figure S2. $^{31}P\{^{1}H\}$ NMR (162 MHz, CD_2Cl_2, 25 °C) spectrum of complex **1**.

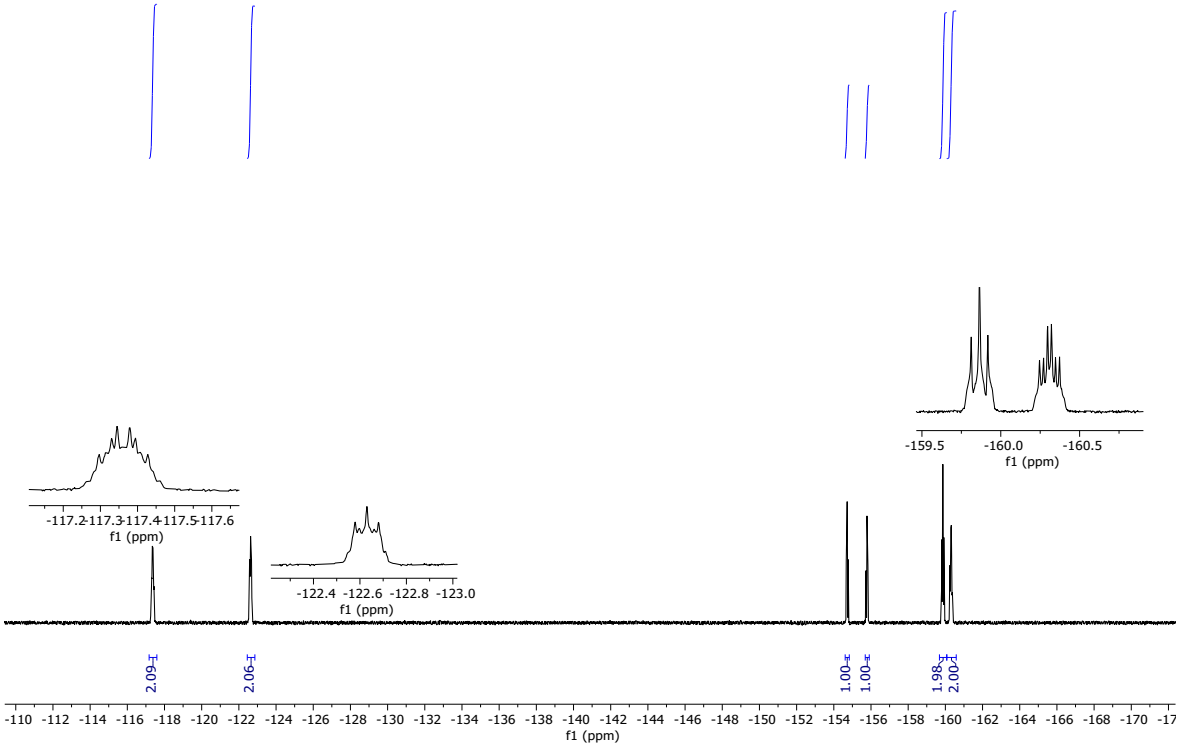

Figure S3. ^{19}F NMR (376 MHz, CD_2Cl_2, 25 °C) spectrum of complex **1**.

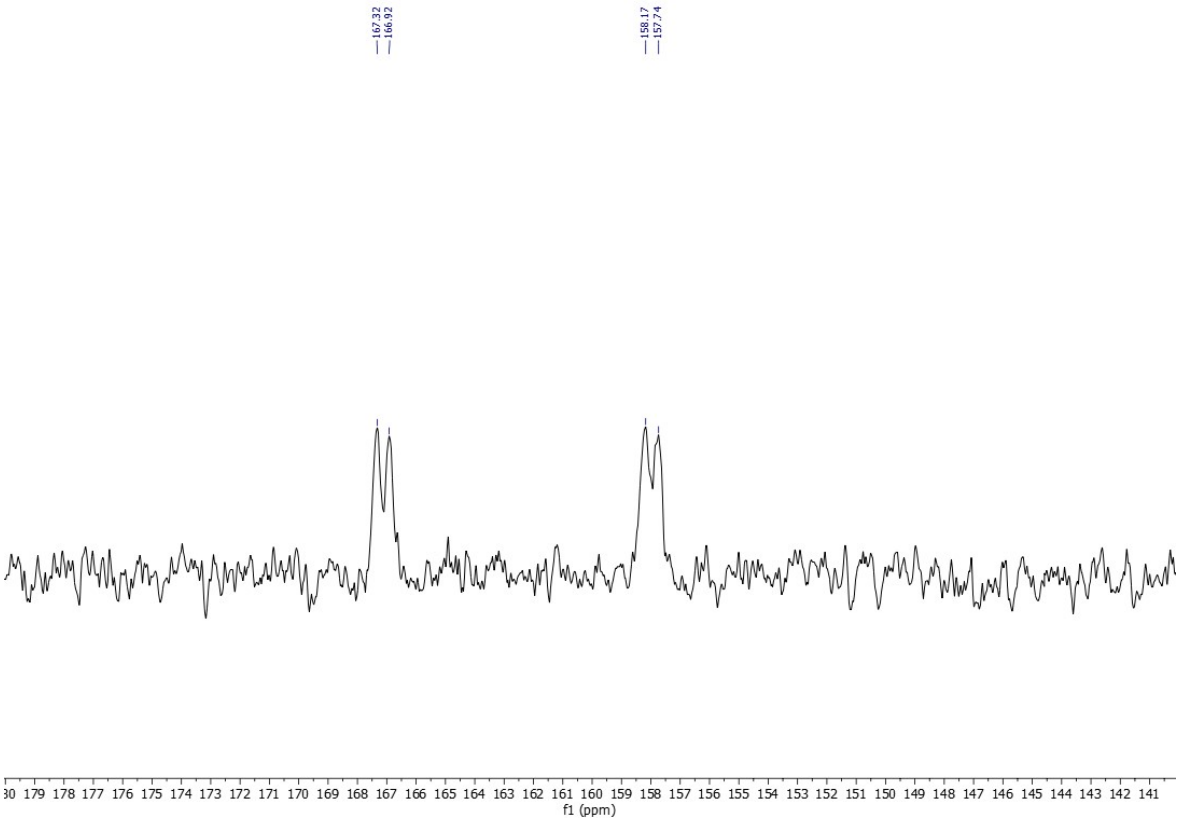

Figure S4. ^{125}Te NMR (126 MHz, CD_2Cl_2, 25 °C) spectrum of complex **1**.

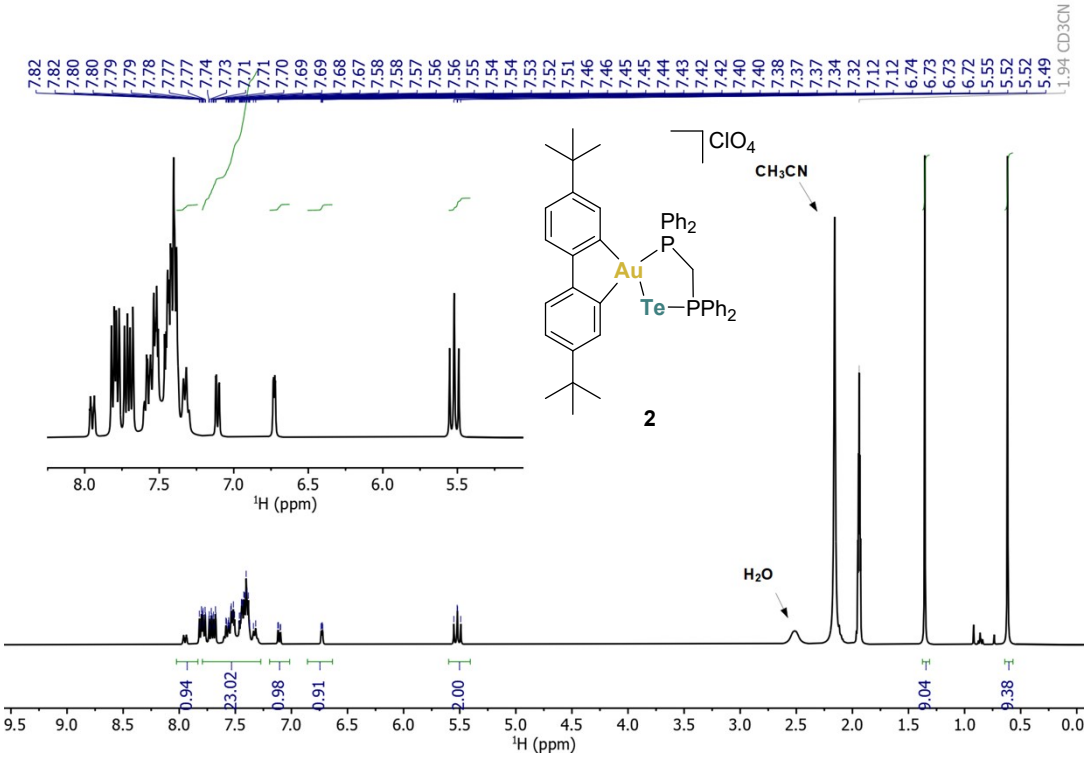

Figure S5. ^{1}H NMR (400 MHz, CD_3CN, 25 °C) spectrum of complex **2**.

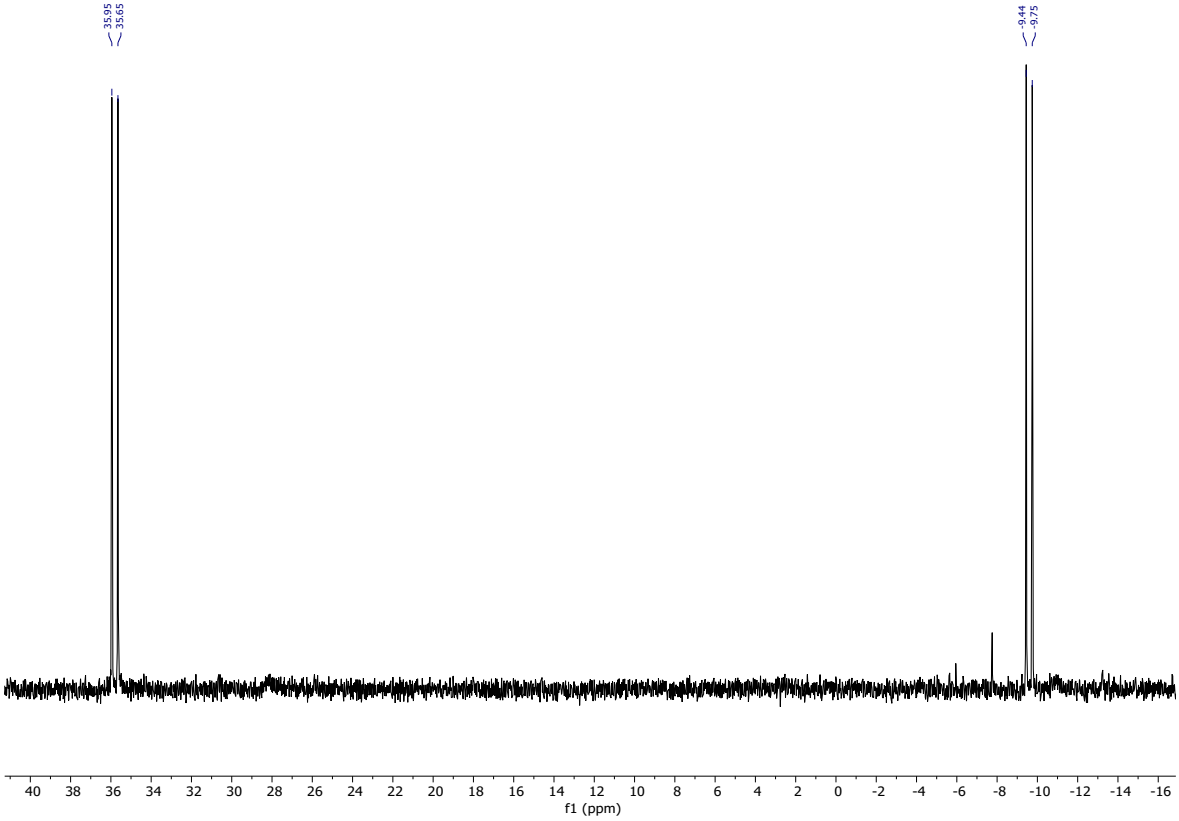

Figure S6. $^{31}P\{^{1}H\}$ NMR (162 MHz, CD_3CN, 25 °C) spectrum of complex **2**.

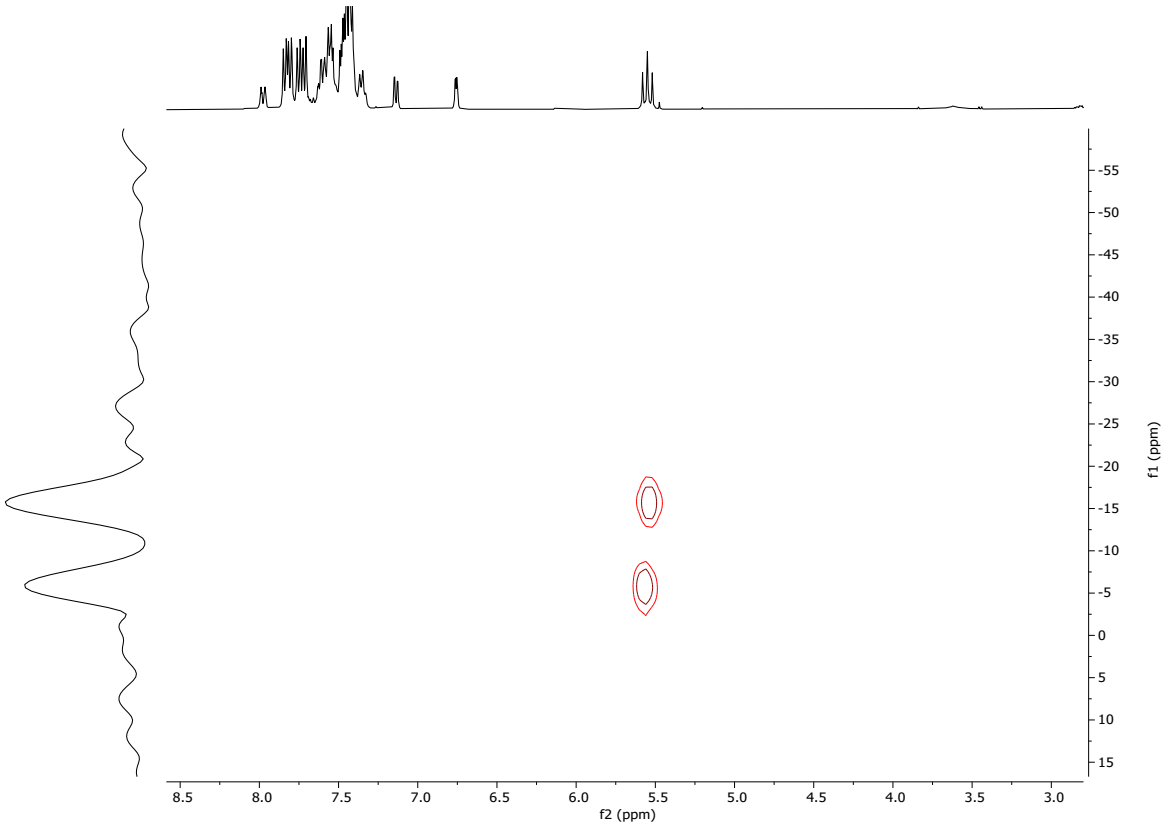

Figure S7. HMQC ^{1}H–^{125}Te NMR (^{1}H 400 MHz, ^{125}Te 126 MHz, CD_3CN, 25 °C) spectrum of complex **2**.

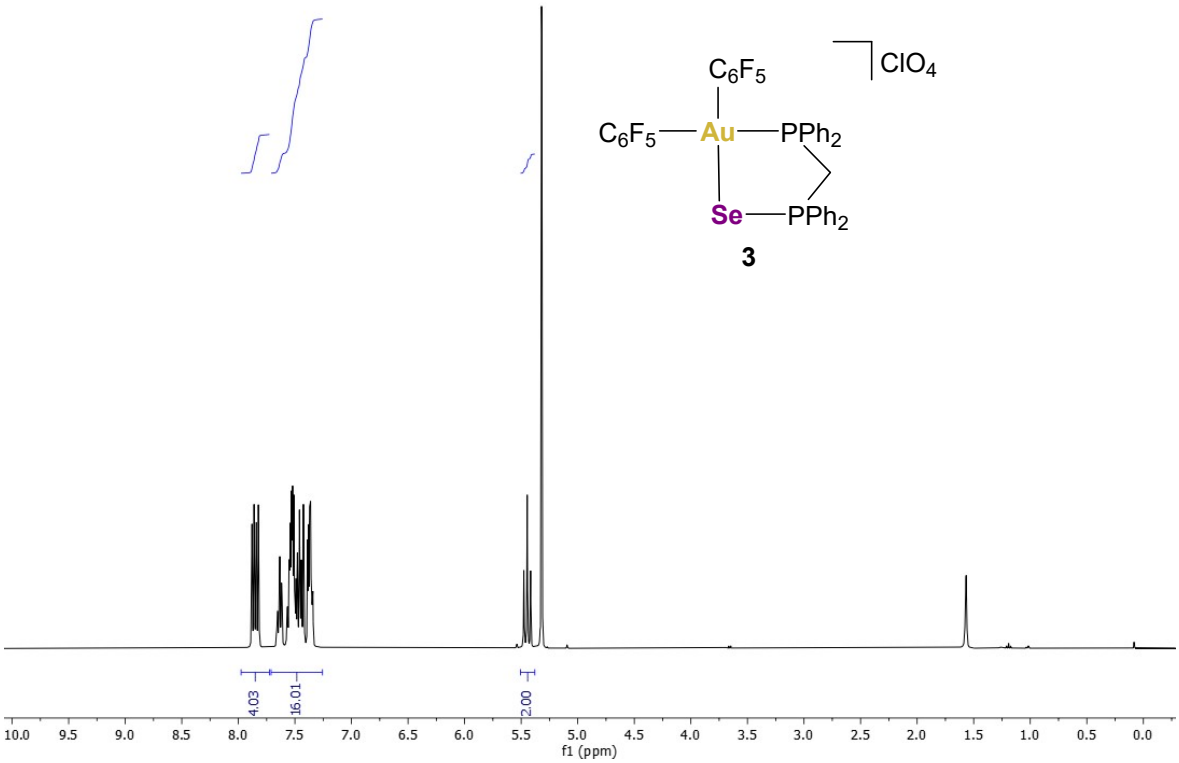

Figure S8. ^{1}H NMR (400 MHz, CD_2Cl_2, 25 °C) spectrum of complex **3**.

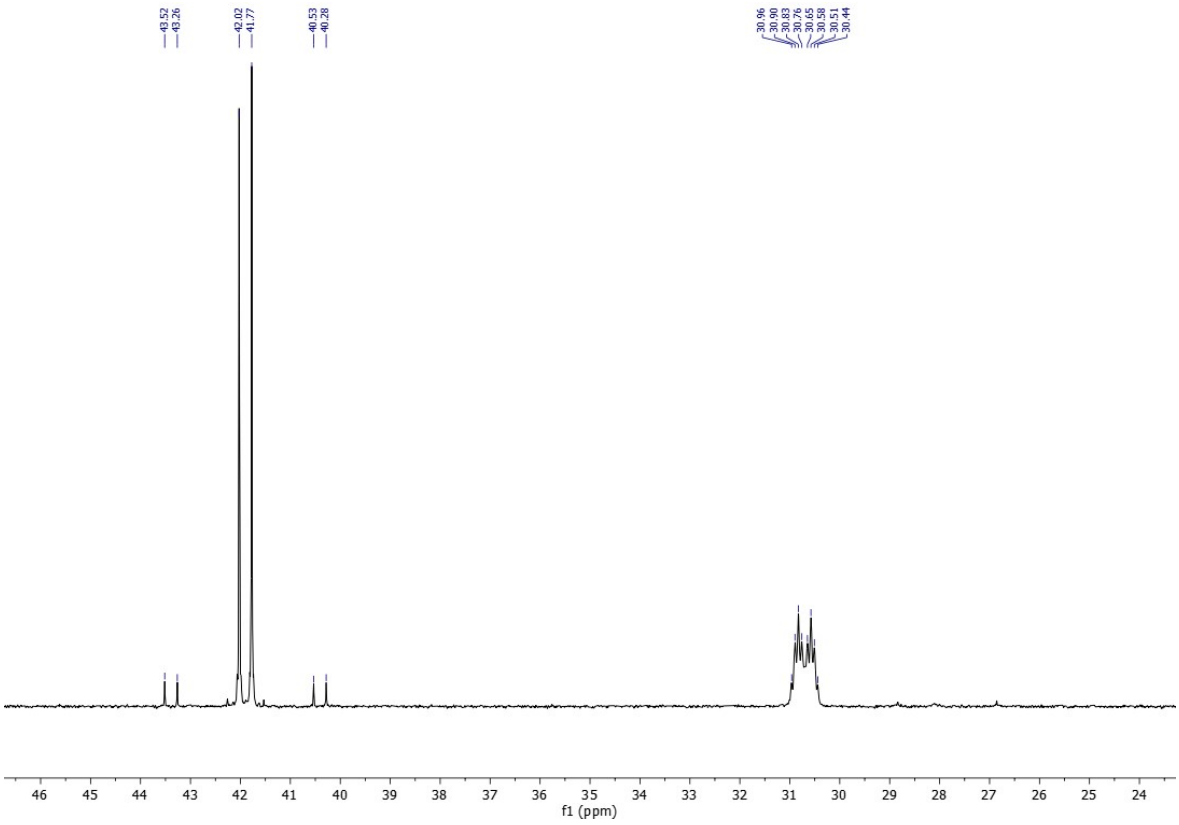

Figure S9. $^{31}P\{^{1}H\}$ NMR (162 MHz, CD_2Cl_2, 25 °C) spectrum of complex **3**.

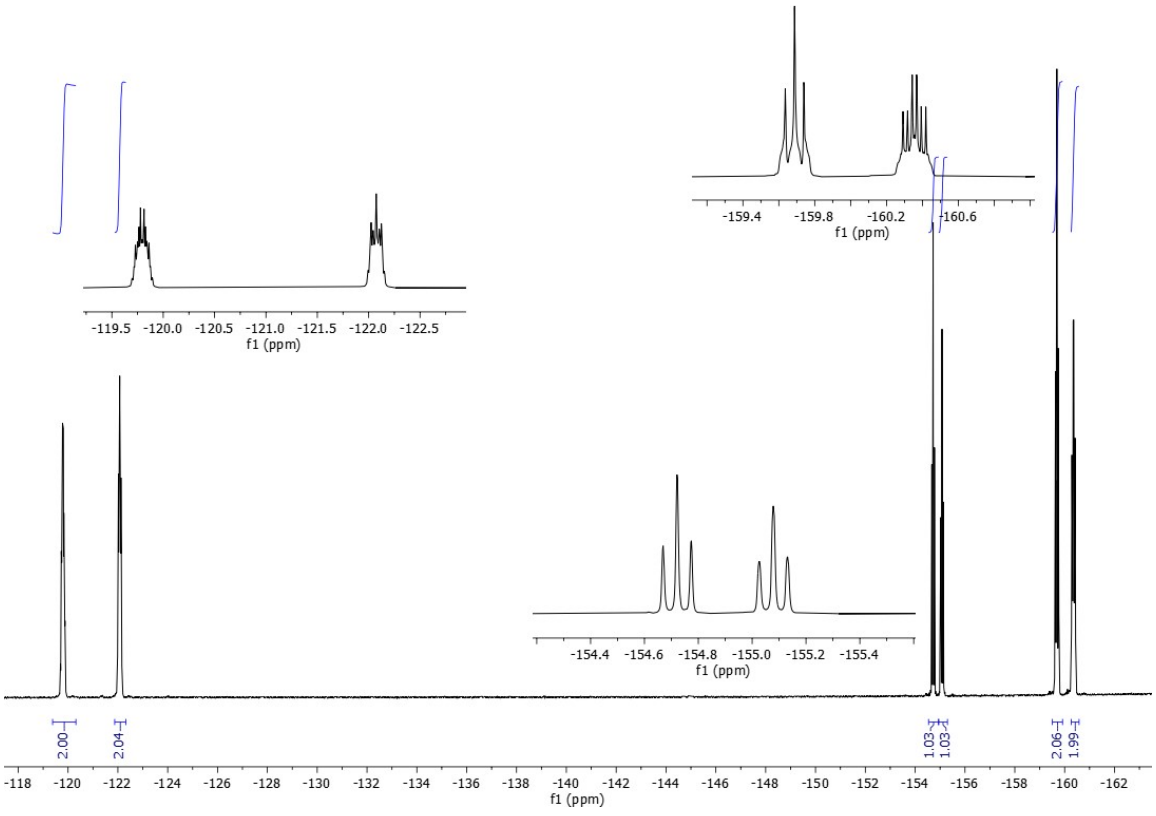

Figure S10. ^{19}F NMR (376 MHz, CD_2Cl_2, 25 °C) spectrum of complex **3**.

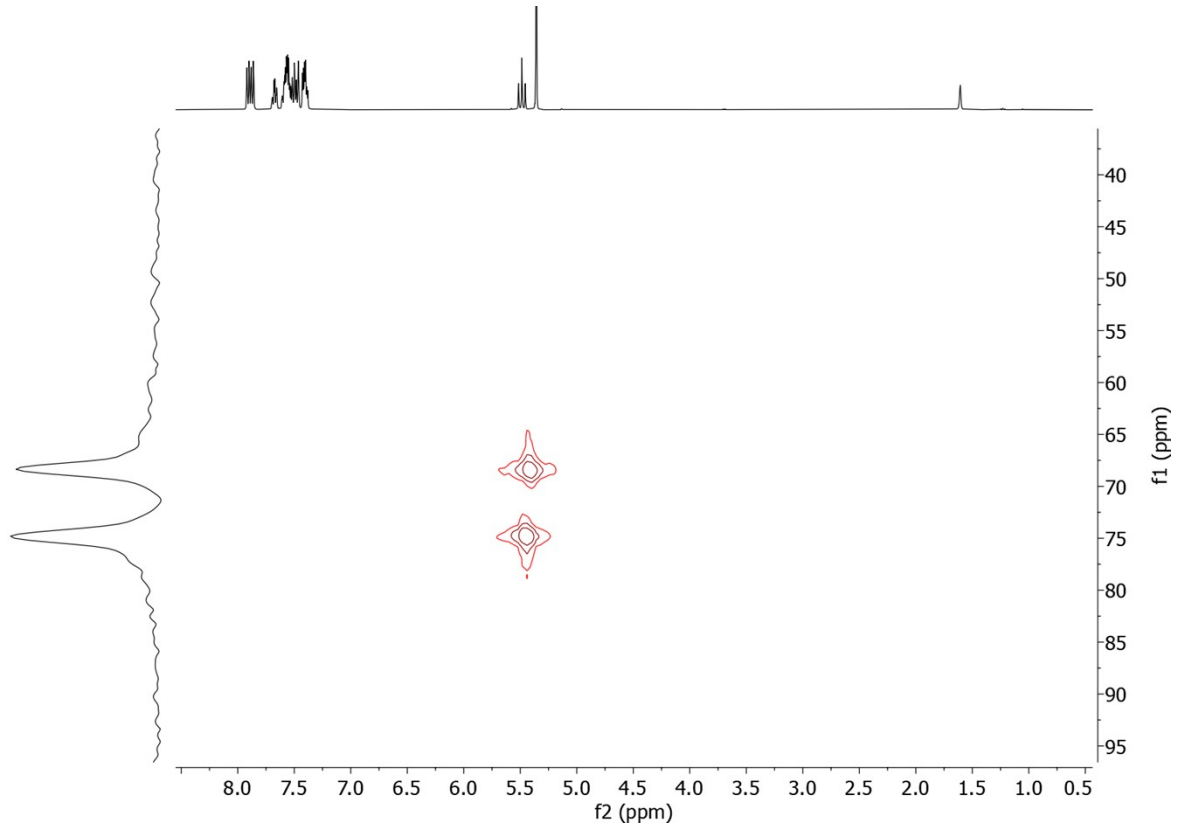

Figure S11. HMQC ^{1}H–^{77}Se NMR (^{1}H 400 MHz, ^{77}Se 76 MHz, CD_2Cl_2, 25 °C) spectrum of complex **3**.

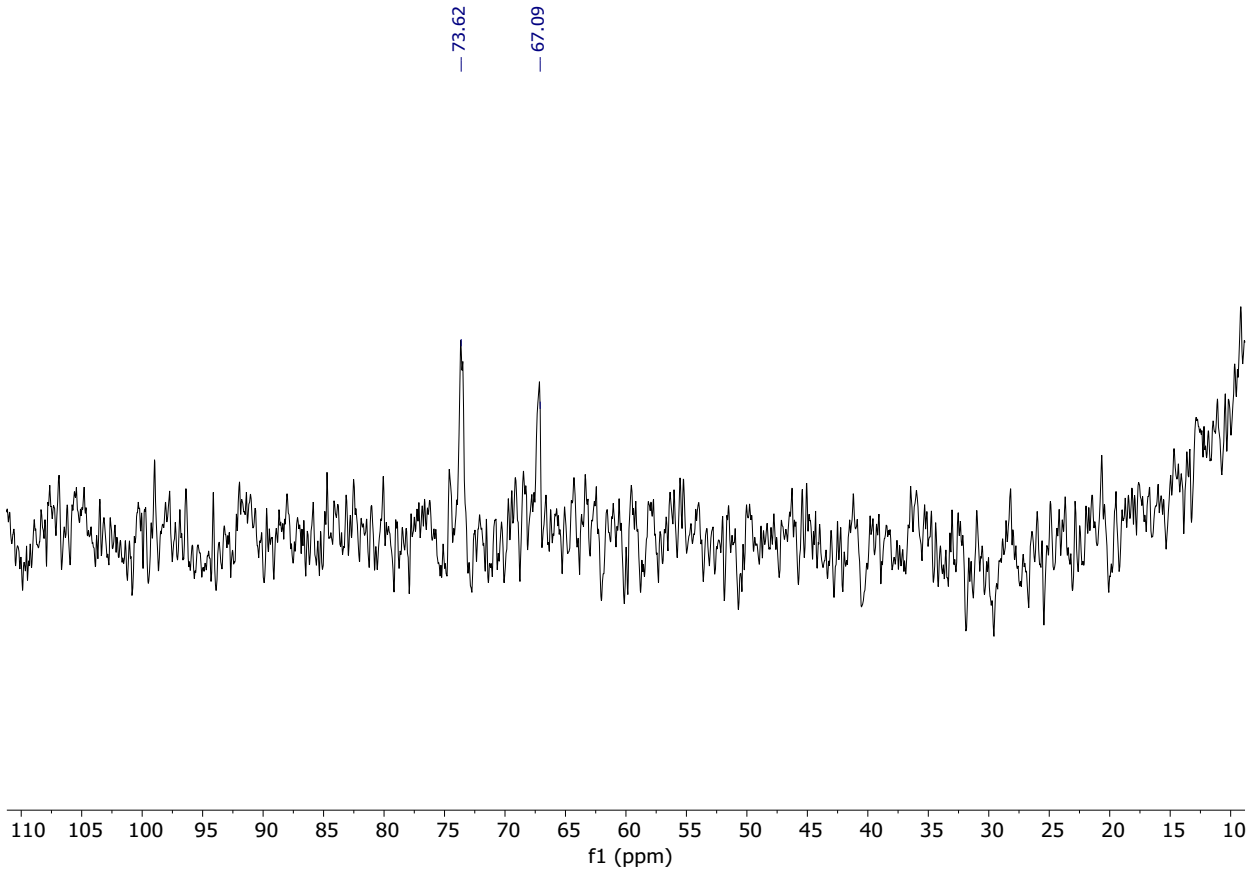

Figure S12. ^{77}Se NMR (76 MHz, CD_2Cl_2, 25 °C) spectrum of complex **3**.

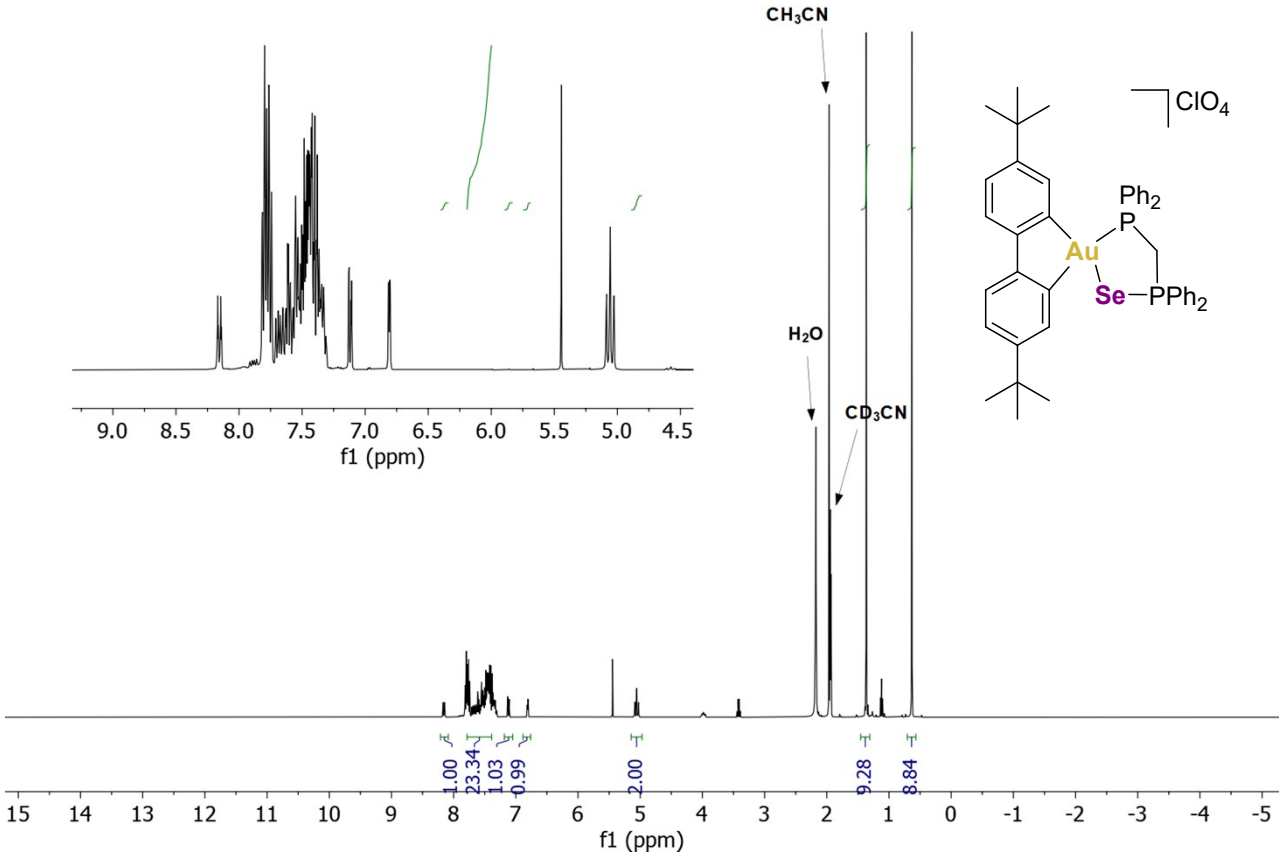

Figure S13. ^{1}H NMR (400 MHz, CD_3CN, 25 °C) spectrum of complex **4**.

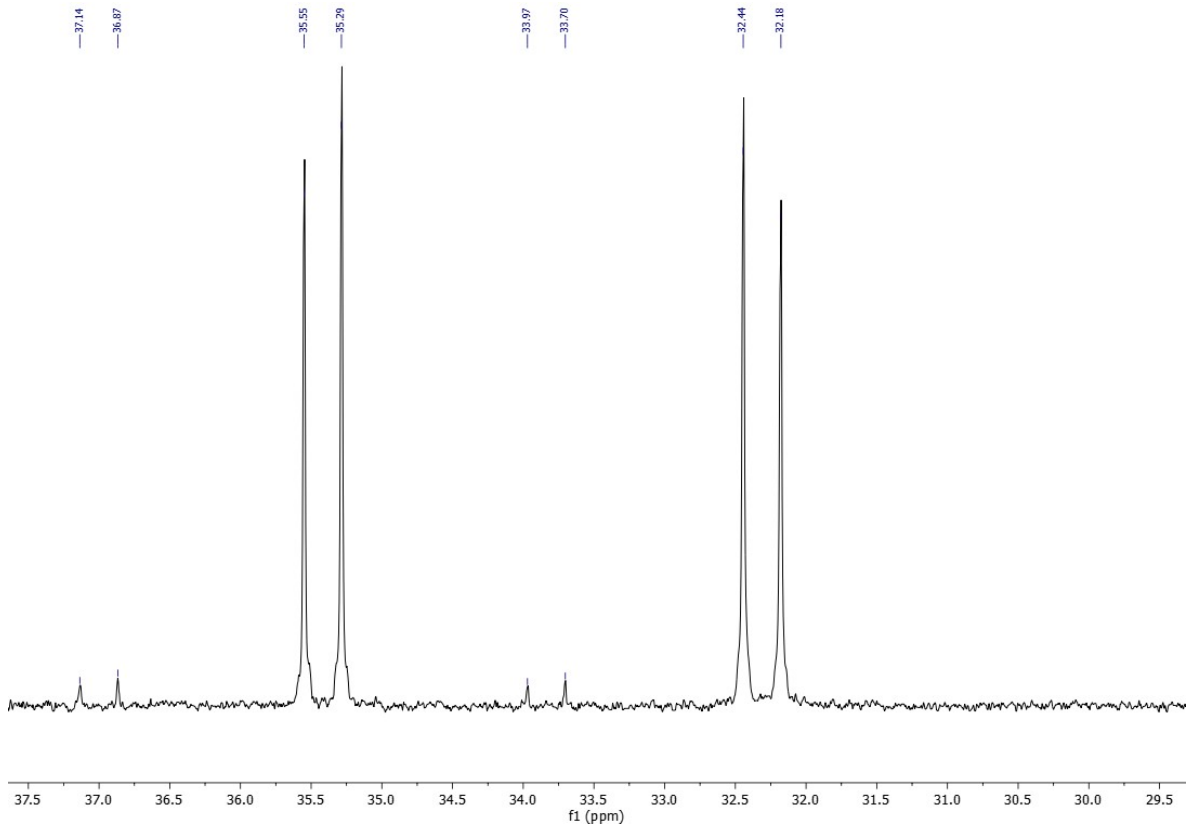

Figure S14. $^{31}P\{^{1}H\}$ NMR (162 MHz, CD_3CN, 25 °C) spectrum of complex **4**.

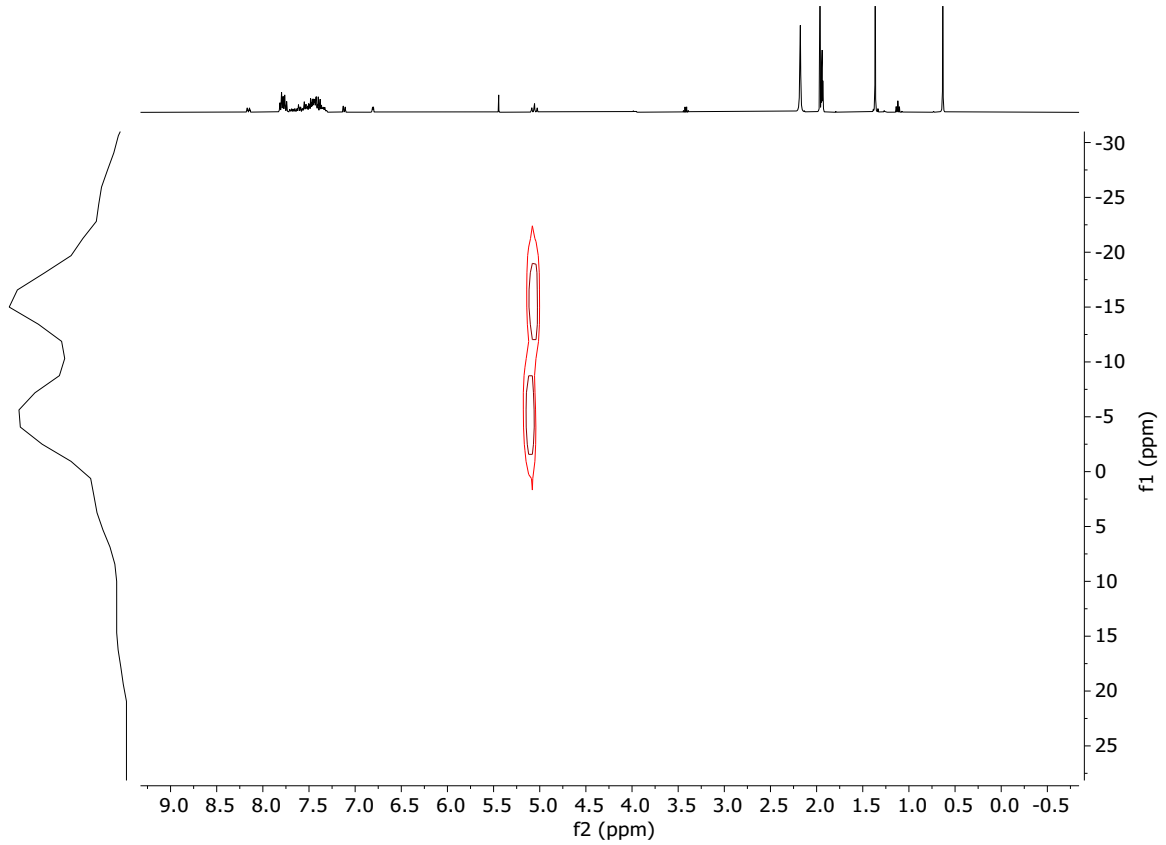

Figure S15. HMQC ^{1}H–^{77}Se NMR (^{1}H 400 MHz, ^{77}Se 76 MHz, CD_2Cl_2, 25 °C) spectrum of complex **4**.

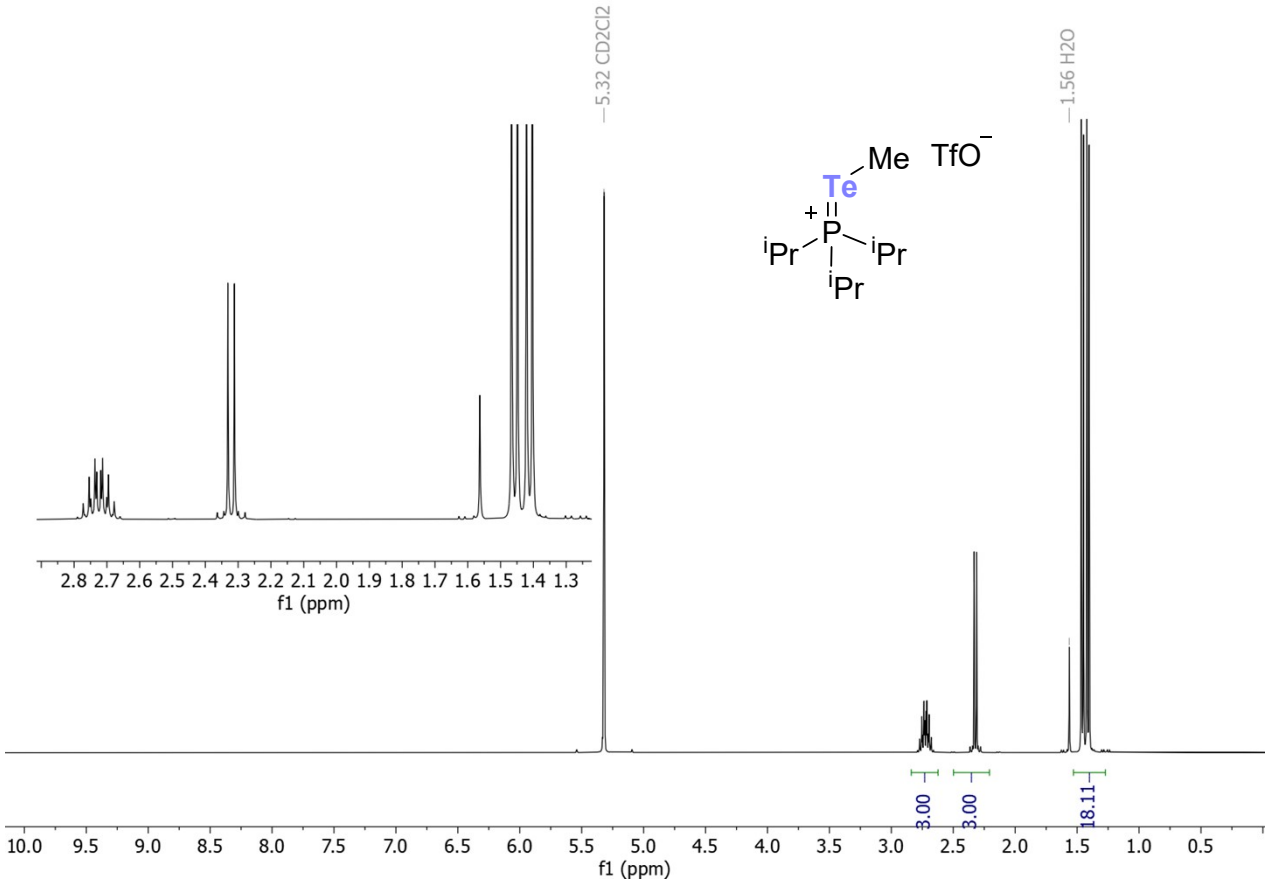

Figure S16. ^{1}H NMR (400 MHz, CD_2Cl_2, 25 °C) spectrum of compound **5**.

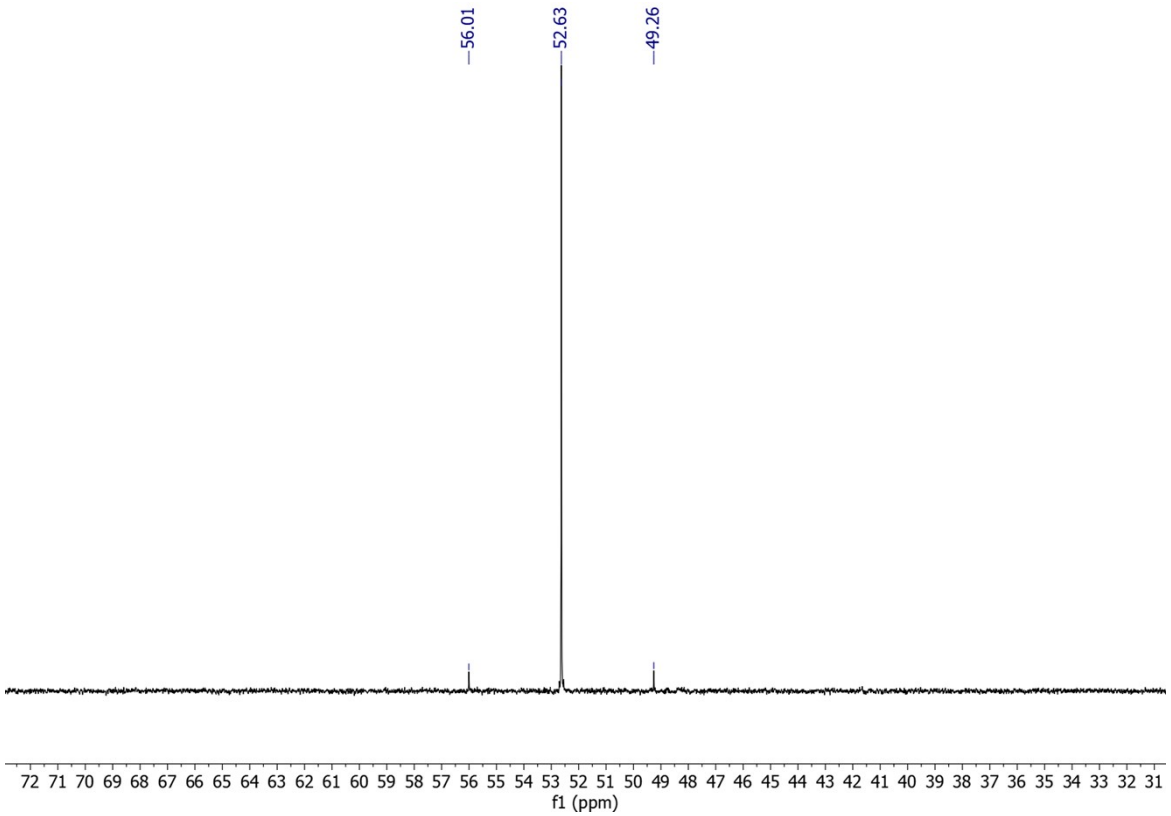

Figure S17. $^{31}P\{^{1}H\}$ NMR (162 MHz, CD_2Cl_2, 25 °C) spectrum of compound **5**.

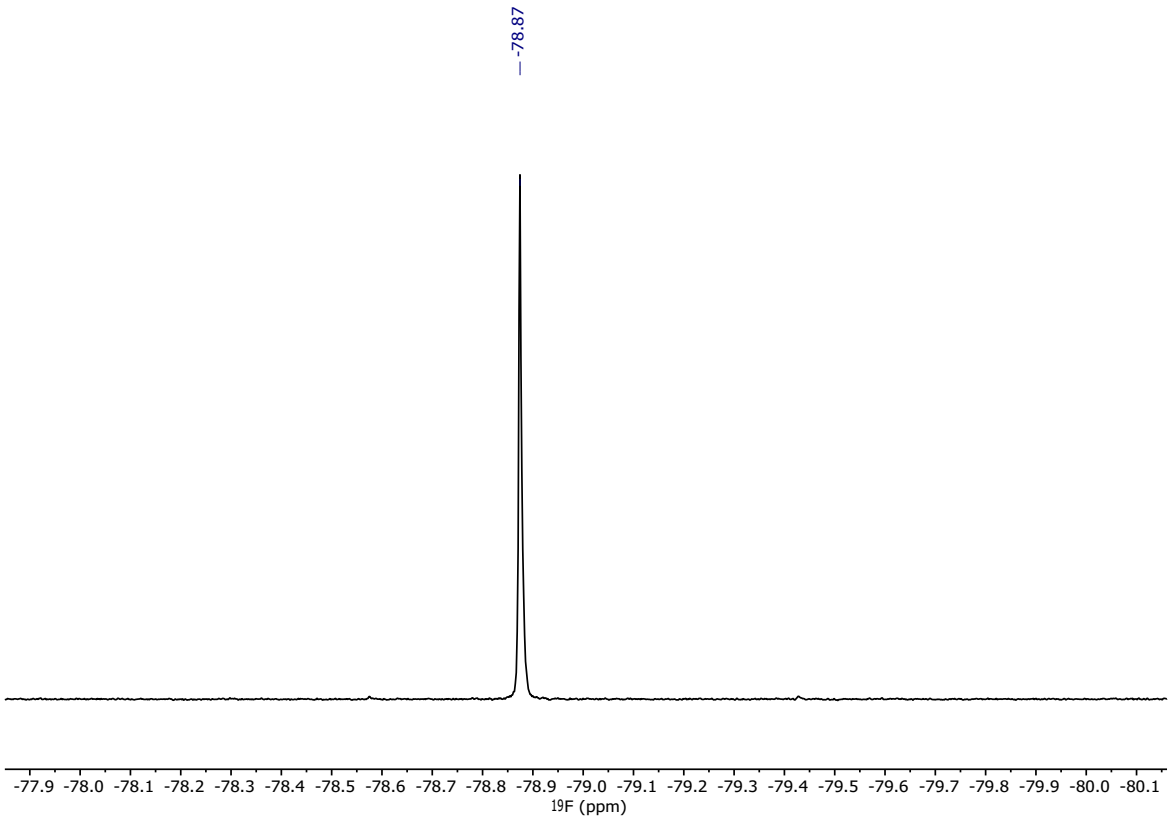

Figure S18. ^{19}F NMR (376 MHz, CD_2Cl_2, 25 °C) spectrum of compound **5**.

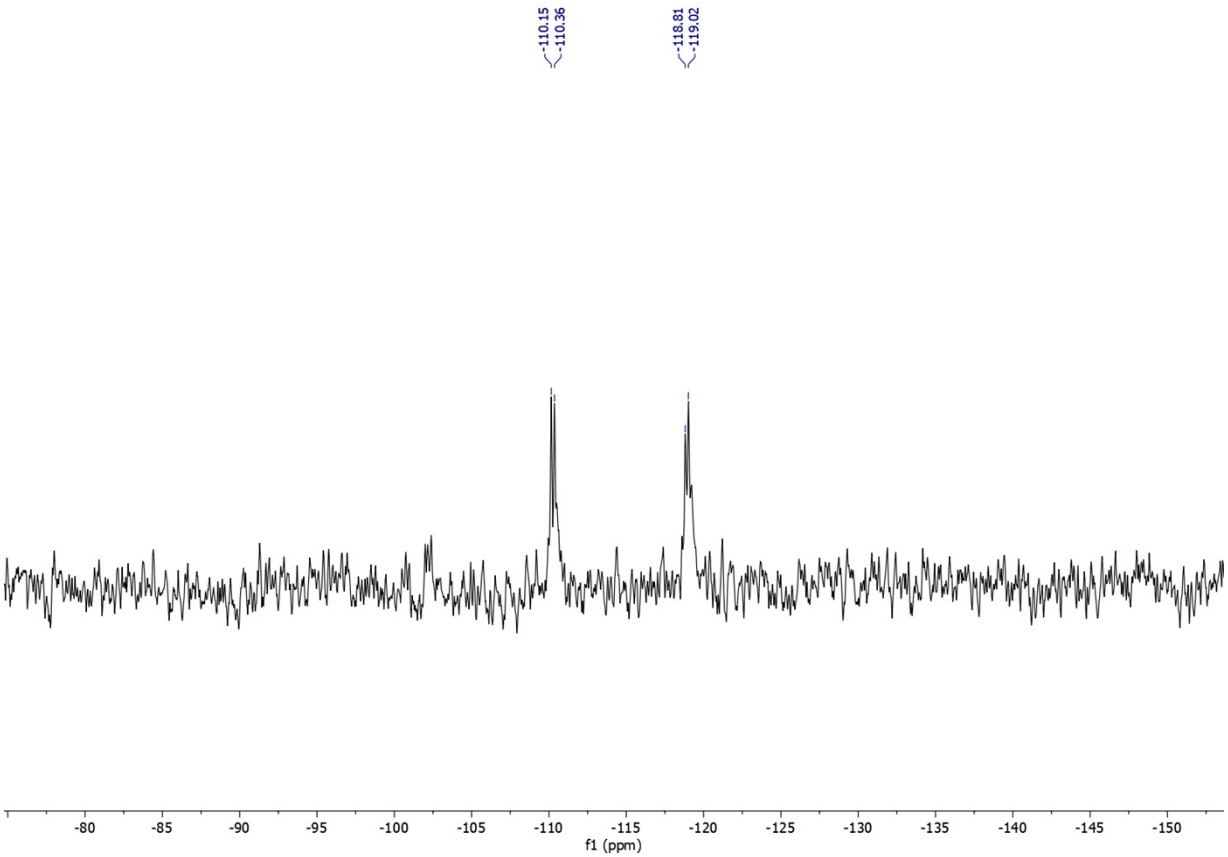

Figure S19. ^{125}Te NMR (126 MHz, CD_2Cl_2, 25 °C) spectrum of compound **5**.

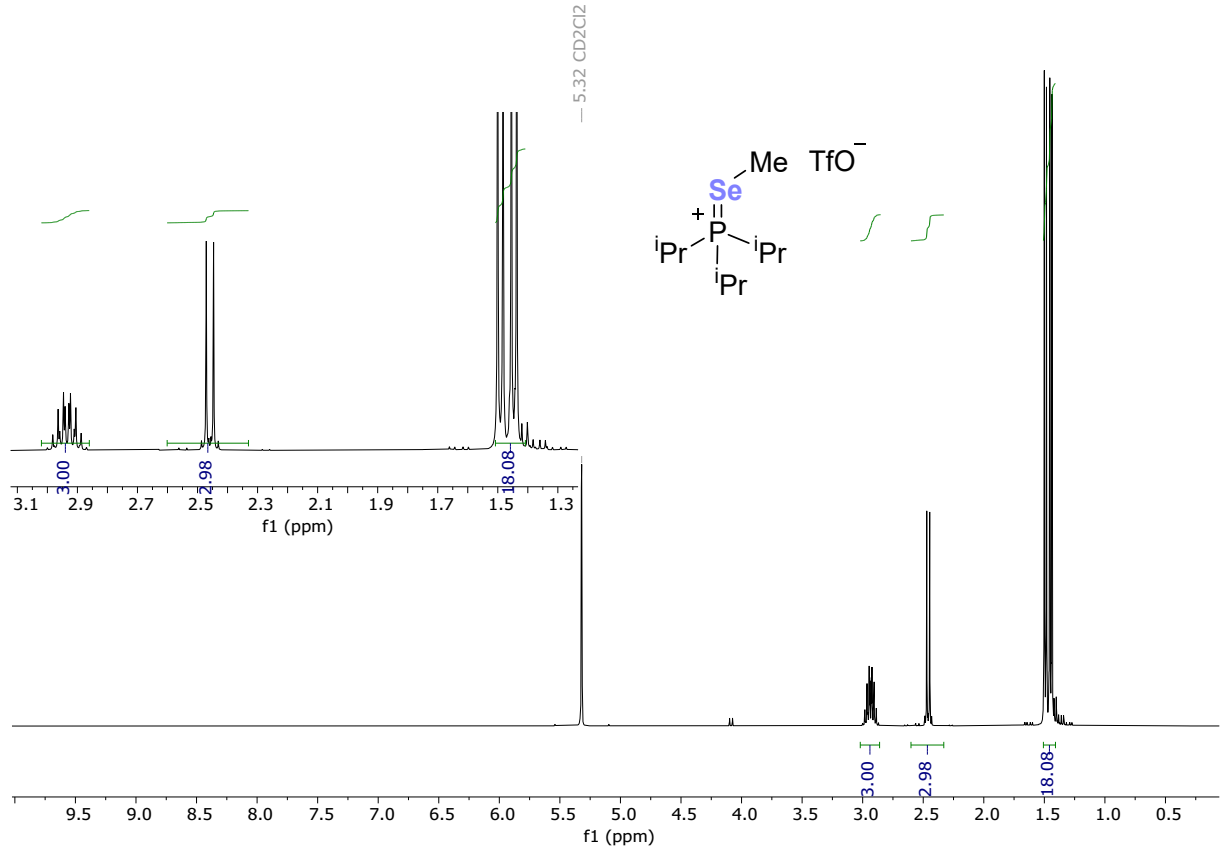

Figure S20. ^{1}H NMR (400 MHz, CD_2Cl_2, 25 °C) spectrum of compound **6**.

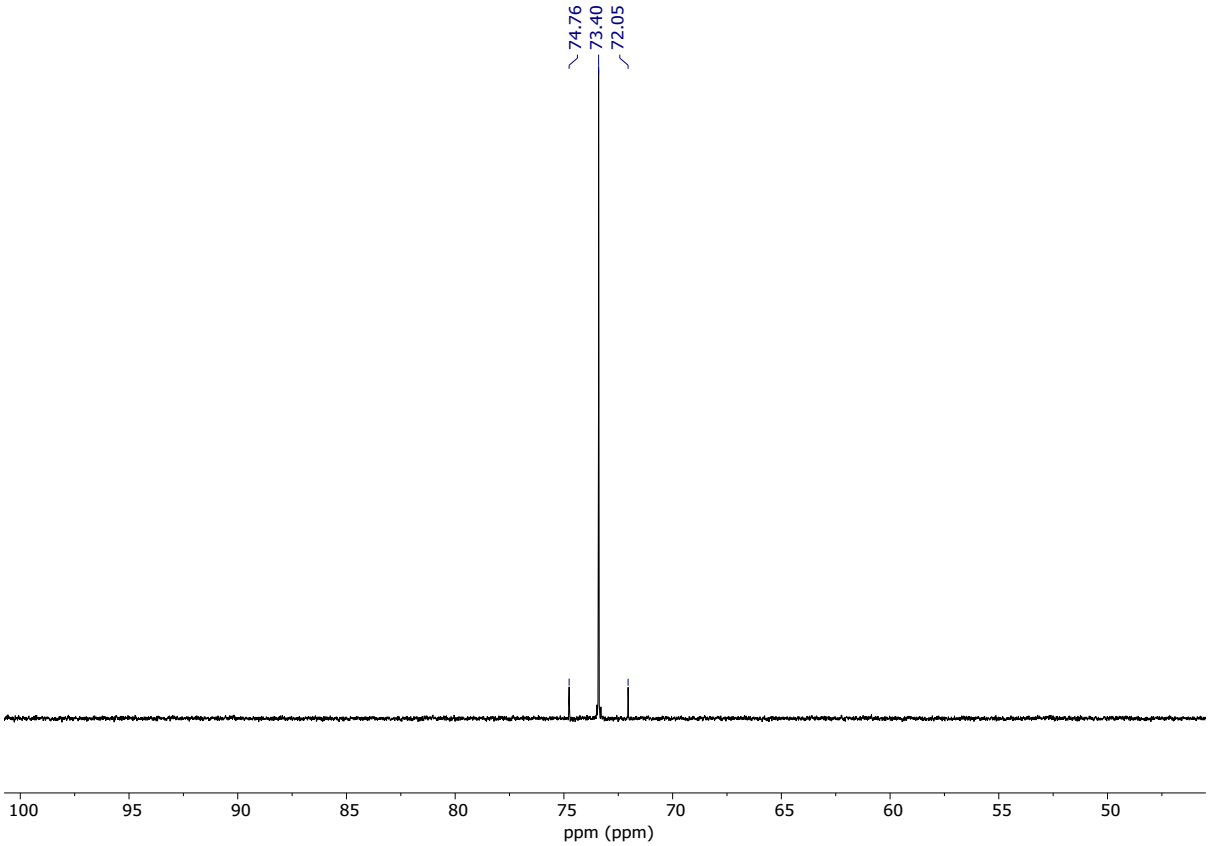

Figure S21. $^{31}P\{^{1}H\}$ NMR (162 MHz, CD_2Cl_2, 25 °C) spectrum of compound **6**.

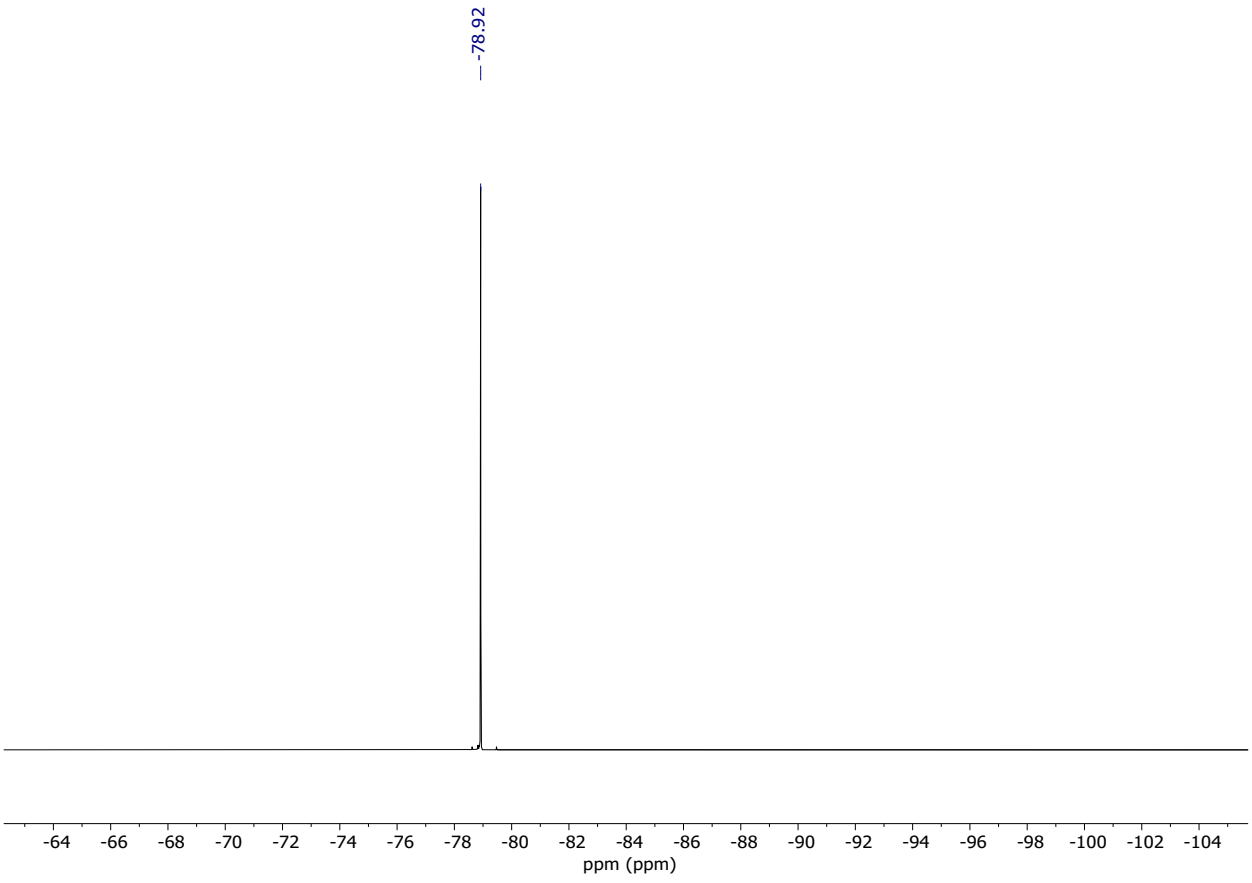

Figure S22. ^{19}F NMR (376 MHz, CD_2Cl_2, 25 °C) spectrum of compound **6**.

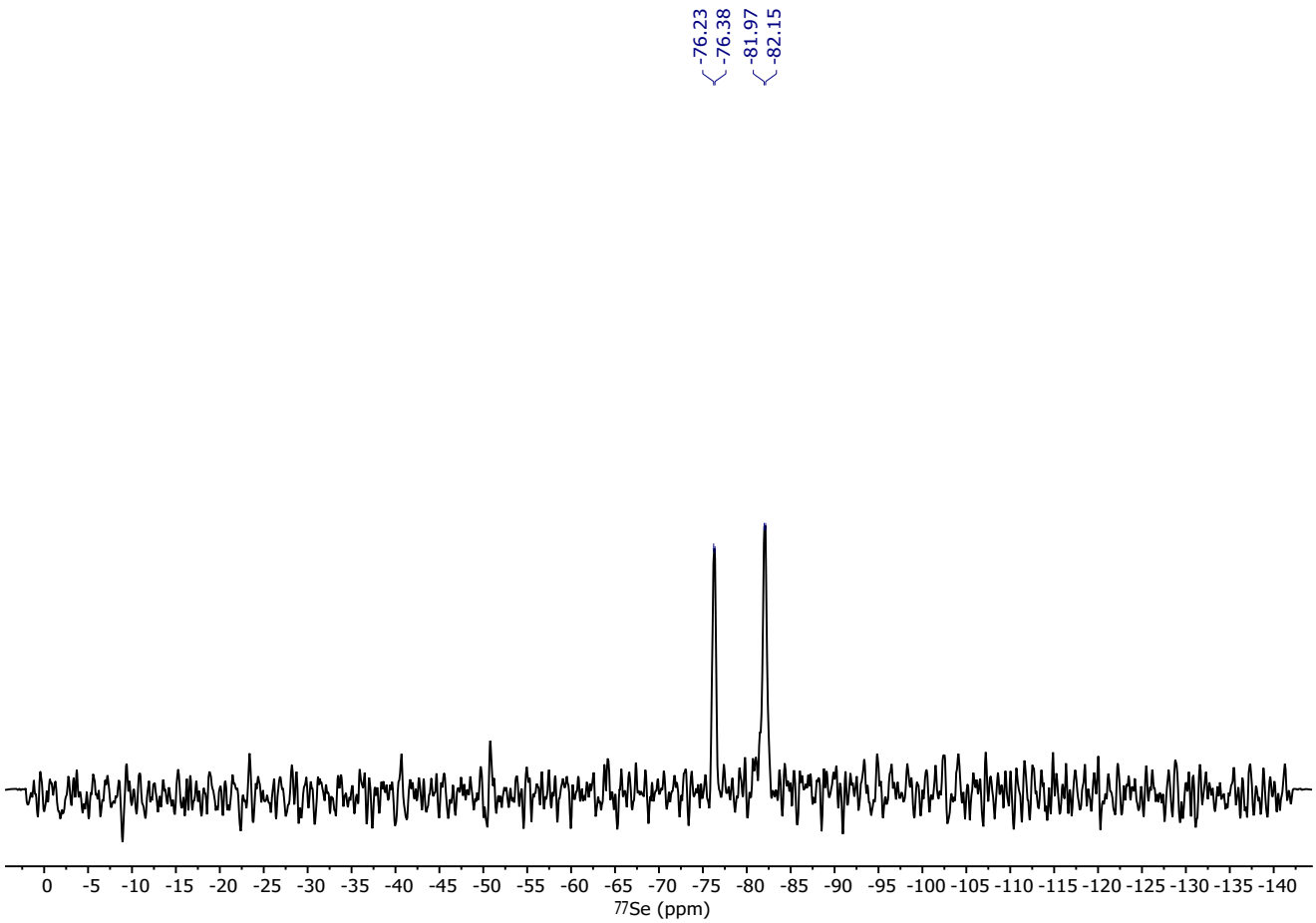

Figure S23. ^{77}Se NMR (76 MHz, CD_2Cl_2, 25 °C) spectrum of compound **6**.

Mechanistic Investigations on Complex 1 Formation (Variable Temperature NMR)

Complex $[Au(C_6F_5)_2(dppm)][ClO_4]$ (25.38 mg, 0.025 mmol) and $TeP(^iPr)_3$ (7.20 mg, 0.025 mmol) were placed in a J Young® NMR tube and cooled to ca. –80 °C. Subsequently, CD_2Cl_2 (0.6 mL) was slowly added along the wall of the NMR tube to ensure gradual cooling before reaching the NMR tube's bottom. A pale-yellow solution was obtained, which was allowed to cool for 5 minutes. Then, the NMR tube was inserted into a precooled probe (–80 °C) and the reaction progress was monitored through variable temperature ^1H, $^{31}P\{^1H\}$ and ^{19}F NMR.

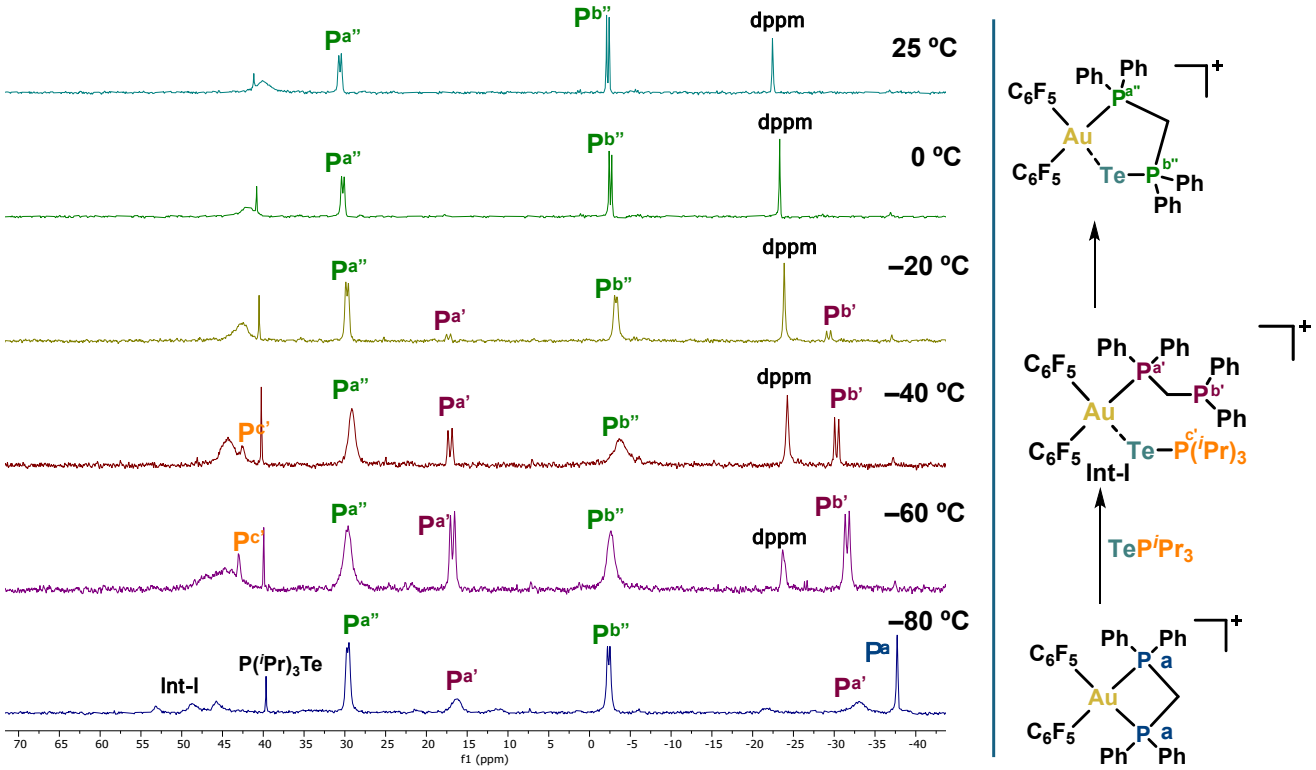

Figure S24. Variable temperature $^{31}P\{^1H\}$ NMR (162 MHz, CD_2Cl_2) spectra of an equimolecular mixture of $[Au(C_6F_5)_2(dppm)][ClO_4]$ and $Te(P^iPr_3)$, showing the formation of product **1** via a proposed intermediate **Int-I**.

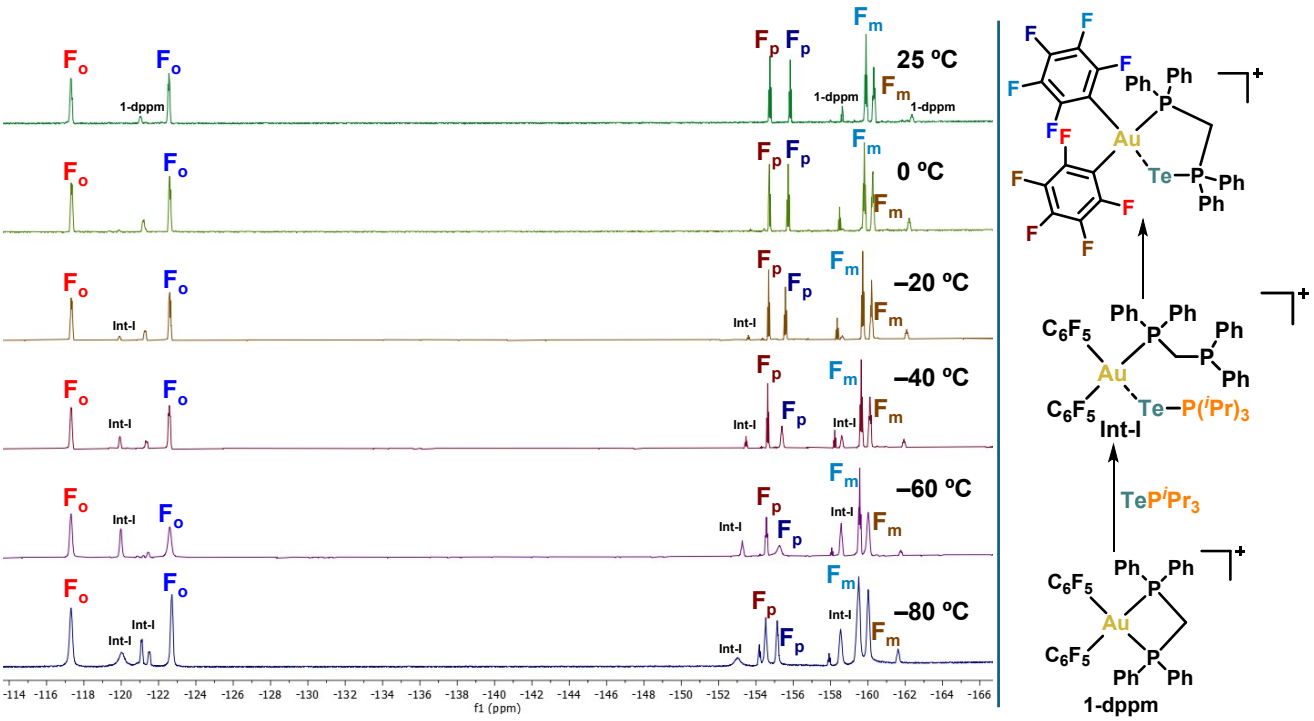

Figure S25. Variable temperature ^{19}F NMR (376 MHz, CD_2Cl_2) spectra of an equimolecular mixture of $[Au(C_6F_5)_2(dppm)][ClO_4]$ and Te(P^iPr_3), showing the formation of product **1** via a proposed intermediate **Int-I**.

4. Catalytic Studies

General procedure: In a 5 mL scintillation vial, 2-phenylquinoline (0.010 mmol) and the corresponding complex were dissolved in $CDCl_3$ (0.500 mL). Hantzsch ester (0.022 mmol, 2.2 equiv) was then added, affording a pale-yellow solution. The reaction mixture was stirred at room temperature for 3 h. The resulting solution was transferred to an NMR tube, and conversion was determined by ^1H NMR integration of diagnostic resonances of the substrate and product.

Catalyst addition at low loadings: For reactions performed at 1.0 mol%, a stock solution of compound **5** was prepared in $CDCl_3$ (10 mg in 1.00 mL). The appropriate aliquot of this stock solution was dispensed using a calibrated micropipette to deliver the desired catalyst amount.

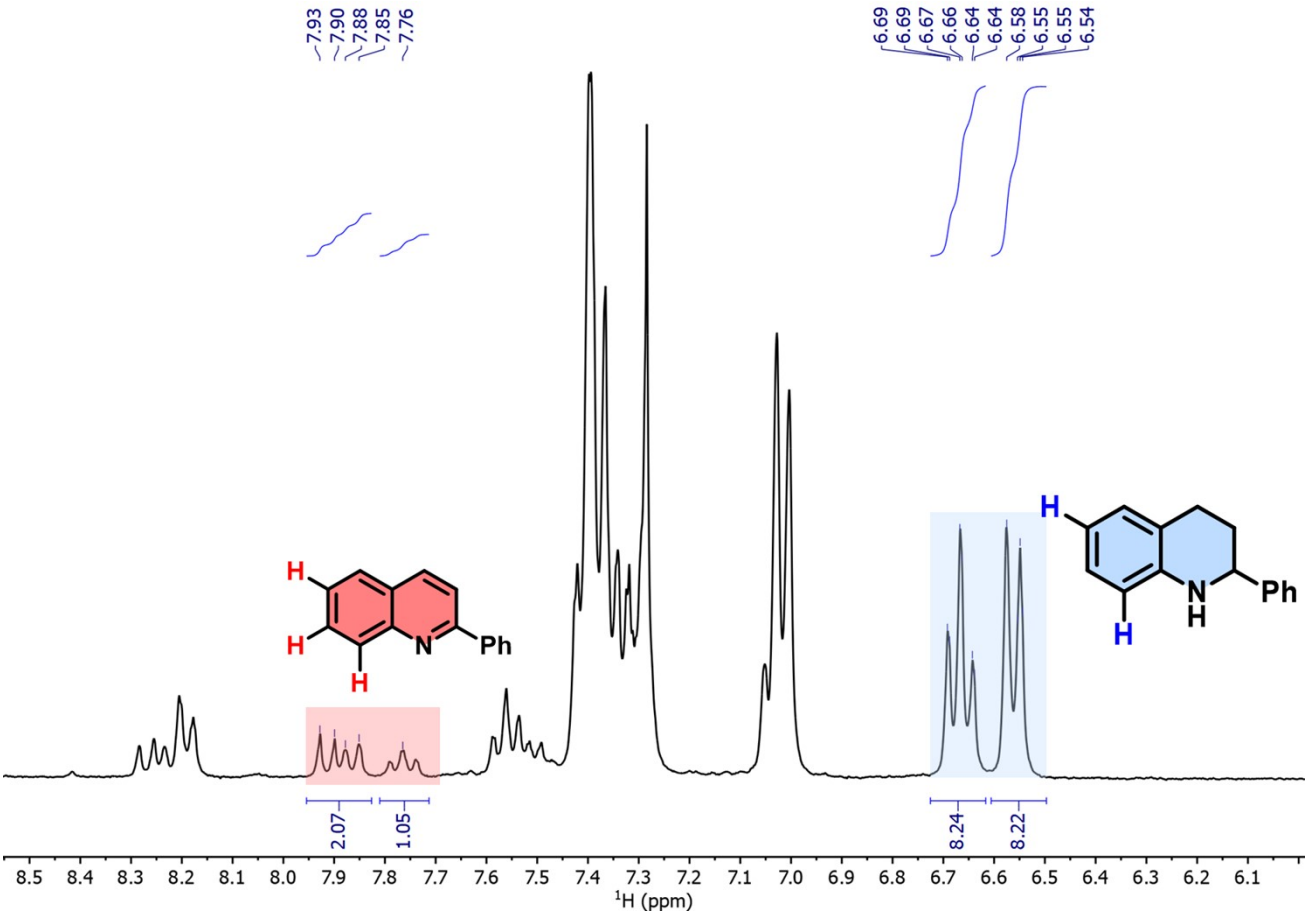

Figure S27. ^1H NMR ($CDCl_3$, 300 MHz) of one catalytic run ([**Te**] = **5**) after 3 h showing the characteristic signals integrated.

5. Crystal Data and Structure Refinement

Table S1. Crystal data and structure refinement for complex **1**.

Empirical Formula	$C_{79}\,H_{53}\,O_8\,Au_2\,Cl_2\,F_{20}\,P_4\,Te_2$
M_t [g·mol^{-1}]	2354.12
Crystal system	Triclinic
Space group	P-1
a [Å]	11.8837(4)
b [Å]	19.1816(7)
c [Å]	19.4735(6)
α [°]	75.1630(10)
β [°]	86.3620(10)
γ [°]	72.6990(10)
V [Å^3]	4096.4
Z, Z'	Z = 2, Z' = 1
Density [g·cm^{-3}]	1.909
T [K]	100(2)
μ [mm^{-1}]	4.518
F(000)	2254.0
2θ range [°]	3.972 to 56.606
no. of collected reflections	236000
no. of unique reflections	20326
R_{int}	0.0414
R_1, wR_2 [$I > 2\sigma(I)$][a]	$R_1 = 0.0222$, $wR_2 = 0.0554$
R_1, wR_2 (all data)[a]	$R_1 = 0.0232$, $wR_2 = 0.0557$
GOF (F^2)[b]	1.026

[a] $R_1 = \Sigma(|F_o| - |F_c|) / \Sigma |F_o|$. $wR_2 = [\Sigma w (F_o^2 - F_c^2)^2 / \Sigma w(F_o^2)^2]^{1/2}$

[b] Goodness-of-fit = $[\Sigma w (F_o^2 - F_c^2)^2 / (n_{obs} - n_{param})]^{1/2}$

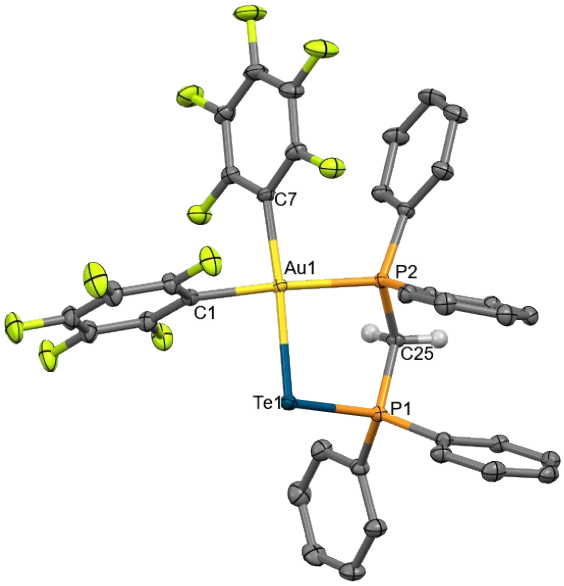

Table S2. Interatomic distances [Å] and angles [°] for complex **1** (one of two molecules, hydrogen atoms, perchlorate anion and an *n*-hexane molecule are omitted for clarity) with atom labelling as indicated above.

Au1–Te1	2.5956(4)	Au1–Te1–P1	96.06(2)
P1–Te1	2.4290(6)	C1–Au1–Te1	85.83(7)
Au1–C1	2.069(2)	C1–Au1–C7	91.09(1)
Au1–C7	2.055(3)	C7–Au1–P2	93.06(7)
Au1–P2	2.3319(6)	P2–Au1–Te1	90.09(2)
		Te1–P1–C25	107.32(8)
		P2–C25–P1	110.30(1)
		C25–P2–Au1	106.94(8)

Table S3. Crystal data and structure refinement for complex **3**.

Empirical Formula	$C_{37}\ H_{22}\ O_4\ Au\ Cl\ F_{10}\ P_2\ Se$
M_t [g·mol^{-1}]	1093.86
Crystal system	Triclinic
Space group	P-1
a [Å]	9.4400(7)
b [Å]	11.6453(8)
c [Å]	18.9697(15)
α [°]	73.133(3)
β [°]	81.267(3)
γ [°]	71.046(3)
V [Å^3]	1883.6(2)
Z, Z'	Z = 2, Z' = 1
Density [g·cm^{-3}]	1.929
T [K]	100(2)
μ [mm^{-1}]	5.117
F(000)	1052.0
2θ range [°]	4.496 to 56.648
no. of collected reflections	87924
no. of unique reflections	9362
R_{int}	0.0520
R_1, wR_2 [I > 2σ(I)][a]	R1 = 0.0167, wR2 = 0.0394
R_1, wR_2 (all data)[a]	R1 = 0.0186, wR2 = 0.0397
GOF (F^2)[b]	1.027

[a] $R_1 = \Sigma(|F_o| - |F_c|) / \Sigma |F_o|$. $wR_2 = [\Sigma w (F_o^2 - F_c^2)^2 / \Sigma w(F_o^2)^2]^{1/2}$

[b] Goodness-of-fit = $[\Sigma w (F_o^2 - F_c^2)^2 / (n_{obs} - n_{param})]^{1/2}$

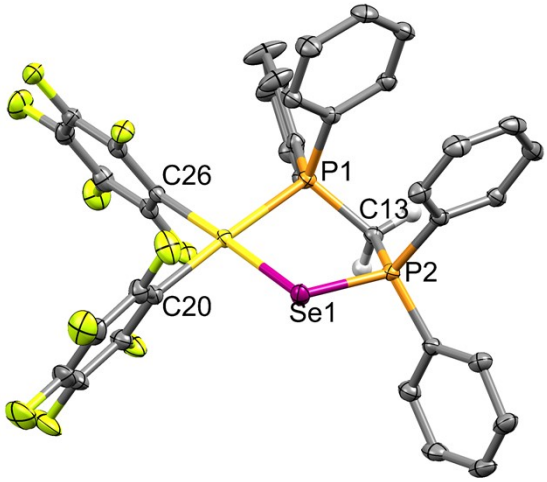

Table S4. Interatomic distances [Å] and angles [°] for complex **3** (hydrogen atoms and perchlorate anion are omitted for clarity) with atom labelling as indicated above.

Au1–Se1	2.4568(4)	Au1–Se1–P1	96.07(2)
P1–Se1	2.4287(6)	C20–Au1–Se1	85.82(7)
Au1–C20	2.069(2)	C20–Au1–C26	91.10(1)
Au1–C26	2.055(3)	C26–Au1–P1	93.07(7)
Au1–P1	2.3318(6)	P1–Au1–Se1	90.09(2)
		Se1–P2–C13	107.33(8)
		P2–C13–P1	110.30(1)
		C26–P2–Au1	106.94(8)

Table S5. Crystal data and structure refinement for compound **5**.

Empirical Formula	$C_{11}\ H_{24}\ O_3\ F_3\ S\ Te\ P$
M_t [g·mol^{-1}]	451.93
Crystal system	Monoclinic
Space group	$P2_1/n$
a [Å]	8.4358(2)
b [Å]	22.2637(5)
c [Å]	9.2066(2)
α [°]	90
β [°]	96.8510(10)
γ [°]	90
V [Å^3]	1716.76(7)
Z, Z'	Z = 4, Z' = 1
Density [g·cm^{-3}]	1.749
T [K]	100(2)
μ [mm^{-1}]	1.979
F(000)	896.0
2θ range [°]	4.818 to 56.626
no. of collected reflections	42742
no. of unique reflections	4263
R_{int}	0.0584
R_1, wR_2 [I > 2σ(I)][a]	R_1 = 0.0164, wR_2 = 0.0392
R_1, wR_2 (all data)[a]	R_1 = 0.0213, wR_2 = 0.0398
GOF (F^2)[b]	1.031

[a] $R_1 = \Sigma(|F_o| - |F_c|) / \Sigma |F_o|$. $wR_2 = [\Sigma w (F_o^2 - F_c^2)^2 / \Sigma w(F_o^2)^2]^{1/2}$

[b] Goodness-of-fit = $[\Sigma w (F_o^2 - F_c^2)^2 / (n_{obs} - n_{param})]^{1/2}$

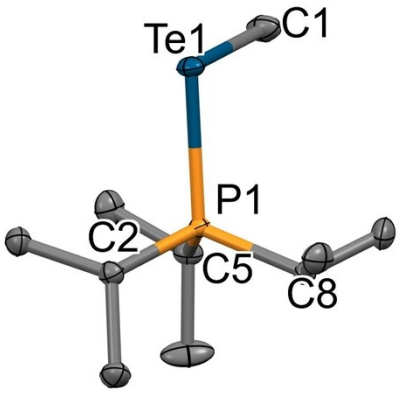

Table S6. Interatomic distances [Å] and angles [°] for compound **5** (hydrogen atoms and triflate anion are omitted for clarity) with atom labelling as indicated above.

P1–Te1	2.4487(3)	P1–Te1–C1	96.07(2)
P1–C2	1.832(1)	C2–P1–C8	107.97(6)
P1–C5	1.837(1)	C8–P1–C5	107.36(6)
P1–C8	1.828(1)	C2–P1–C5	115.31(6)
Te1–C1	2.148(2)		

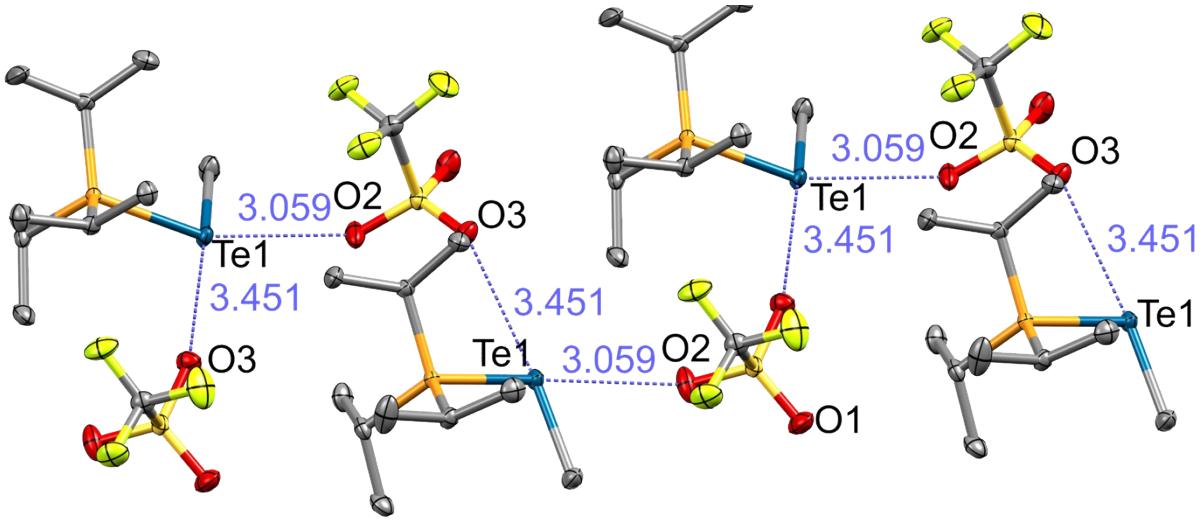

Figure S26. Supramolecular assembly of **5** showing bidentate Te···O chalcogen-bonding interactions with triflate counteranions.

6. Computational Details

Computational chemistry calculations

DFT mechanistic studies were conducted with Gaussian 16.[7] Geometry optimizations were performed at the ωB97X-D[8,9]/def2SVP[10,11] level of theory. Vibrational frequency calculations were used to confirm that stationary points were minima on the potential energy surface and to obtain frequencies used to calculate thermochemistry values with the GoodVibes[12] program. Electronic energies were refined using the ωB97X-D/def2QZVPP method. In all cases, the calculations included the integral equation formalism variant of the polarizable continuum model (IEF-PCM)[13,14] with the SMD[15] solvation model (solvent=dichloromethane) to account for solvent effects.

AQME automated workflows. AQME[16] was used to automate the creation, analysis, and refinement of DFT inputs and outputs. The following workflows were executed:

Conformer generation. The standard RDKit-based conformer search implemented in AQME (sampling + filtering + clustering up to a maximum of 25 structures) was employed for individual molecules. The command line used was:

" python -m aqme --csearch --program rdkit --input Au-Te.csv "

The input Au-Te.csv file contained the following columns:

code_name	SMILES	charge	mult	complex_type
Te-PiPr3	[Te-][P+](C(C)C)(C(C)C)C(C)C	0	1	
PiPr3	CC(C)P(C(C)C)C(C)C	0	1	
Au_init_complex	FC1=C(F)C(F)=C(F)C(F)=C1[Au]2([P+](C3=CC=CC=C3)(C[P+]2(C4=CC=CC=C4)C5=CC=CC=C5)C6=CC=CC=C6)C7=C(F)C(F)=C(F)C(F)=C7F	1	1	squareplanar
Int-I	FC1=C(F)C(F)=C(F)C(F)=C1[Au]([Te][P+](C(C)C)(C(C)C)C(C)C)(C2=C(F)C(F)=C(F)C(F)=C2F)[P+](C3=CC=CC=C3)(CP(C4=CC=CC=C4)C5=CC=CC=C5)C6=CC=CC=C6	1	1	squareplanar
1	FC1=C(F)C(F)=C(F)C(F)=C1[Au]2(C3=C(F)C(F)=C(F)C(F)=C3F)[P+](C4=CC=CC=C4)(C[P+](C5=CC=CC=C5)([Te]2)C6=CC=CC=C6)C7=CC=CC=C7	1	1	squareplanar

Analysis of Gaussian output files. Outputs from geometry optimizations were pre-processed to ensure normal terminations. Calculations with errors and imaginary frequencies were automatically identified, corrected, and resubmitted until they achieved normal terminations. The following command line was executed:

" python -m aqme --qcorr --files "*.log" "

Creation of Gaussian input files. Geometries from i) initial conformers and ii) successfully terminated optimizations were automatically retrieved and inserted into Gaussian input files. The command line used was:

- Initial conformers (opt + freq):

“ python -m aqme --qprep --files "*.log" --qm_input "opt freq wb97xd scrf=(smd,solvent=dichloromethane) def2svp" --program gaussian --mem 32GB --nprocs 16 ”

- Single-point energy corrections:

“ python -m aqme --qprep --files "*.log" --qm_input "wb97xd/Def2QZVPP scrf=(solvent=dichloromethane,smd)" --suffix QZ --program gaussian --mem 32GB --nprocs 16 ”

Molecular coordinates and energy of the associative intermediate.

Energy of the intermediate: -4205.517566 a.u.

Energy of the most stable Int-I: -4205.561531 a.u.

ΔE vs Int-I: 0.043965 a.u. (27.6 kcal·mol^{-1})

Molecular coordinates:

C -6.28552300 0.68886300 -2.19927600
C -4.90068000 0.17489700 -2.60604800
C -5.01029100 -1.00385800 -3.57618400
P -3.74712000 -0.20145400 -1.20369300
C -4.24294200 -1.71955900 -0.26310400
C -5.74766800 -1.80351100 0.00833300
C -3.73439600 -3.02845700 -0.86876200
C -3.65962800 1.24482400 -0.04520800
C -3.57906700 2.55861700 -0.82740400
C -4.69731000 1.29344400 1.07784200
Te -1.51536400 -0.44612500 -2.19457400
Au 0.30687500 -0.15658900 -0.03708000
P 1.94006300 1.34307100 -0.99958800
C 3.16942500 0.71142800 -2.16704200
C 4.36041600 0.12222500 -1.72762100
C 5.23061700 -0.44966700 -2.65260000
C 4.91255600 -0.44251200 -4.01062100
C 3.72739000 0.14924200 -4.44903400
C 2.85522900 0.72828500 -3.53124600
C 2.70385000 1.67289800 0.63659000
P 1.17667300 1.55476800 1.67488800
C 1.71400800 1.19129300 3.37295000
C 0.73387700 1.00574400 4.35857200
C 1.10755400 0.73645800 5.67269500
C 2.45751400 0.64812000 6.01426700
C 3.43459600 0.83238300 5.03729400
C 3.06760500 1.10160400 3.71920800
C 0.50080000 3.24650800 1.72817300
C 1.13658100 4.23696600 2.48985200
C 0.66799500 5.54770200 2.45715700
C -0.43566000 5.87530700 1.66705400
C -1.07580300 4.89019200 0.91694200
C -0.61296800 3.57529300 0.95102500
C 1.34854300 2.94424200 -1.62804000
C 2.11496900 4.09734400 -1.41014200
C 1.64813100 5.33328100 -1.84944600
C 0.42703400 5.42408400 -2.51999200
C -0.32663400 4.27566800 -2.75494200
C 0.12854300 3.03741300 -2.30580700
C -0.90835800 -1.32122600 1.16911000
C -1.65798500 -0.72981900 2.18342300
F -1.67099900 0.60045200 2.34984200

C -2.45705000 -1.45384800 3.06267900
F -3.15618300 -0.83039600 4.00268600
C -2.53497300 -2.83568700 2.93264500
F -3.30211300 -3.54438100 3.74567100
C -1.81142600 -3.46182600 1.92387900
F -1.91122400 -4.77379600 1.76183500
C -1.01633200 -2.70578300 1.06410600
F -0.39915500 -3.37854900 0.09668400
C 1.89153700 -1.69231600 -0.23658600
C 2.16572200 -2.28730200 -1.45658800
F 1.44183500 -1.99005000 -2.54476900
C 3.21594800 -3.18109500 -1.63892200
F 3.47057600 -3.70818700 -2.83185400
C 4.02315300 -3.51013600 -0.55411800
F 5.03480000 -4.35395500 -0.70821600
C 3.76887800 -2.94231800 0.69009200
F 4.53948200 -3.25272700 1.72807300
C 2.70604000 -2.05044700 0.82164100
F 2.51682100 -1.51900000 2.04133800
H -6.24759600 1.51923800 -1.48254100
H -6.91242000 -0.10595600 -1.77534000
H -6.79039200 1.06066200 -3.10433500
H -4.36780100 0.99457500 -3.11598500
H -5.58035600 -0.68547300 -4.46219900
H -5.54670700 -1.84856300 -3.11882300
H -4.02721400 -1.36002800 -3.91881900
H -3.71952400 -1.55711100 0.68996400
H -6.17642000 -0.87103700 0.39726100
H -6.29557000 -2.08704700 -0.90221000
H -5.92243300 -2.58947000 0.75912300
H -2.65227500 -3.02119200 -1.04725000
H -3.95513800 -3.84677200 -0.16597700
H -4.23585900 -3.25930100 -1.82004800
H -2.68212400 1.08655300 0.42743900
H -2.76481200 2.54516400 -1.56815600
H -4.51900900 2.79648200 -1.34596200
H -3.37733500 3.37726400 -0.12125700
H -4.65261900 0.41903700 1.74305300
H -5.72611700 1.39393700 0.70287900
H -4.48030200 2.17587100 1.69948000
H 4.60899200 0.08159700 -0.66563100
H 6.15647100 -0.91377000 -2.30667200
H 5.59165900 -0.90204100 -4.73191200
H 3.47739900 0.15646100 -5.51181200
H 1.92398800 1.18271500 -3.87850900
H 3.30980600 0.78550000 0.87632200
H 3.32211500 2.57586600 0.73420200
H -0.32482000 1.07211200 4.10415200
H 0.33717600 0.59231400 6.43316900
H 2.74836900 0.43406700 7.04502700
H 4.49277700 0.76698200 5.29920600
H 3.84892000 1.24442600 2.97047300
H 2.00126700 3.98427300 3.10918800
H 1.16705900 6.31765300 3.04944700
H -0.79987700 6.90467300 1.63884800
H -1.93950500 5.14733600 0.30021700
H -1.10563600 2.80410200 0.35530400
H 3.07294100 4.04298700 -0.88890600
H 2.24067700 6.23141900 -1.66386100
H 0.06254000 6.39641200 -2.85867700
H -1.28207000 4.34191500 -3.27986100
H -0.48405200 2.14497500 -2.45931500

GoodVibes thermochemistry analysis. The reported Gibbs free energies at the ωB97X-D/def2QZVPP//ωB97X-D/def2SVP (SMD, dichloromethane) level of theory were calculated with GoodVibes (v3.0.2). We used this program to introduce quasi-harmonic (QHA) corrections to the computed vibrational entropies using a frequency cut-off value of 100.0 cm^{-1}, following the model proposed by Grimme[17] at 298.15 K. Also, a correction for the change in standard state from gas phase at 1 atm to a 1 M solution was introduced (option "-c 1" in GoodVibes).[18] Entropy corrections due to entropy of mixing, and multi-structural effects (option "--pes") were also included.

All the thermochemical data including absolute energies, zero-point energies (ZPE) and T·S, among other parameters, as well as the absolute energies, corrected final G and relative G, were generated in an automated way using GoodVibes and tabulated in a separate file of the electronic supplementary information (ESI, *Thermochemistry.dat*). Molecular coordinates were generated similarly using the "--xyz" option (*Molecular_coordinates.xyz*). The command line used to run GoodVibes was:

" python -m goodvibes --pes PES.yaml --xyz -c 1 --imag --spc QZ --dup *.log "

7. References

1. R. Usón, A. Laguna, M. Laguna, E. Fernandez, M. D. Villacampa, P. G. Jones and G. M. Sheldrick, Mono, bi-, and tri-nuclear bis(diphenylphosphino)methane gold complexes. Crystal and molecular structures of [bis(diphenylphosphino)methane]bis(pentafluorophenyl)gold(III) perchlorate and 1,2; 2,3-di-μ-[bis(diphenylphosphino)methane]-1,3-dichlorotrigold(I) chlorotris(pentafluorophenyl)aurate(III), *J. Chem. Soc., Dalton Trans.* 1983, 1679-1685.
2. J. Yang, V. Giuso, M.-C. Hou, E. Remadna, J. Forté, H.-C. Su, C. Gourlaouen, M. Mauro and B. Bertrand, Biphenyl Au (III) complexes with phosphine ancillary ligands: Synthesis, optical properties, and electroluminescence in Light-Emitting electrochemical cells, *Inorg. Chem.*, 2023, **62**, 4903–4921.
3. N. Kuhn, G. Henkel, H. Schumann and R. Fröhlich, The Nature of the Bonding in Phosphane Tellurides. An Empirical NMR Study and the Crystal Structure of (iso-$C_3H_7)_3$PTe, *Z. Naturforsch. B* 1990, **45**, 1010–1018.
4. G. M. Sheldrick, SADABS, Software for Empirical Absorption Corrections, 1996.
5. G. M. Sheldrick, Crystal structure refinement with SHELXL, *Acta Crystallogr. Sect. C,* 2015*,* **71**, 3–8.
6. C. F. Macrae, I. Sovago, S. J. Cottrell, P. T. A. Galek, P. McCabe, E. Pidcock, M. Platings, G. P. Shields, J. S. Stevens, M. Towler and P. A. Wood, Mercury 4.0: from visualization to analysis, design and prediction, *J. Appl. Crystallogr.*, 2020, **53**, 226–235.
7. Gaussian 16, Revision C.01, M. J. Frisch, G. W. Trucks, H. B. Schlegel, G. E. Scuseria, M. A. Robb, J. R. Cheeseman, G. Scalmani, V. Barone, G. A. Petersson, H. Nakatsuji, X. Li, M. Caricato, A. V. Marenich, J. Bloino, B. G. Janesko, R. Gomperts, B. Mennucci, H. P. Hratchian, J. V. Ortiz, A. F. Izmaylov, J. L. Sonnenberg, D. Williams-Young, F. Ding, F. Lipparini, F. Egidi, J. Goings, B. Peng, A. Petrone, T. Henderson, D. Ranasinghe, V. G. Zakrzewski, J. Gao, N. Rega, G. Zheng, W. Liang, M. Hada, M. Ehara, K. Toyota, R. Fukuda, J. Hasegawa, M. Ishida, T. Nakajima, Y. Honda, O. Kitao, H. Nakai, T. Vreven, K. Throssell, J. A. Montgomery, Jr., J. E. Peralta, F. Ogliaro, M. J. Bearpark, J. J. Heyd, E. N. Brothers, K. N. Kudin, V. N. Staroverov, T. A. Keith, R. Kobayashi, J. Normand, K. Raghavachari, A. P. Rendell, J. C. Burant, S. S. Iyengar, J. Tomasi, M. Cossi, J. M. Millam, M. Klene, C. Adamo, R. Cammi, J. W. Ochterski, R. L. Martin, K. Morokuma, O. Farkas, J. B. Foresman, and D. J. Fox, Gaussian, Inc., Wallingford CT, 2016.
8. A. D. Becke, Density-Functional Thermochemistry. V. Systematic Optimization of Exchange-Correlation Functionals, *J. Chem. Phys.* 1997, **107**, 8554–8560.
9. J. D. Chai and M. Head-Gordon, 2008, Long-range corrected hybrid density functionals with damped atom–atom dispersion corrections, *Phys. Chem. Chem. Phys.* **10**, 6615–6620.
10. F. Weigend and R. Ahlrichs, Balanced basis sets of split valence, triple zeta valence and quadruple zeta valence quality for H to Rn: Design and assessment of accuracy, *Phys. Chem. Chem. Phys.* 2005, **7**, 3297–3305.
11. F. Weigend, Accurate Coulomb-fitting basis sets for H to Rn, *Phys. Chem. Chem. Phys*. 2006, **8**, 1057–1065.
12. G. Luchini, J. V. Alegre-Requena, I. Funes-Ardoiz and R. S. Paton, GoodVibes: automated thermochemistry for heterogeneous computational chemistry data, *F1000Research* 2020 **9**, 291.

13. E. Cances, B. Mennucci and J. Tomasi, A new integral equation formalism for the polarizable continuum model: Theoretical background and applications to isotropic and anisotropic dielectrics, *J. Chem. Phys.* 1997, **107**, 3032–3041.
14. J. Tomasi, B. Mennucci and E. Cances, The IEF version of the PCM solvation method: an overview of a new method addressed to study molecular solutes at the QM ab initio level. *J. Mol. Struct. Theochem*. 1999, **464**, 211–226.
15. A. V. Marenich, C. J. Cramer and D. G. Truhlar, Universal Solvation Model Based on Solute Electron Density and on a Continuum Model of the Solvent Defined by the Bulk Dielectric Constant and Atomic Surface Tensions, *J. Phys. Chem. B* 2009, **113**, 6378–6396.
16. J. V. Alegre-Requena, S. V. S. Sowndarya, R. Pérez-Soto, T. M. Alturaifi, and R. S. Paton, AQME: Automated quantum mechanical environments for researchers and educators, *WIREs Comput. Mol. Sci.* 2023, **13**, e1663.
17. S. Grimme, Supramolecular Binding Thermodynamics by Dispersion-Corrected Density Functional Theory, *Chem. Eur. J.* 2012, **18**, 9955–9964.
18. V. S. Bryantsev, M. S. Diallo, and W. A. Goddard III, Calculation of Solvation Free Energies of Charged Solutes Using Mixed Cluster/Continuum Models, *J. Phys. Chem. B* 2008, **112**, 9709–9719.